Mathematical development of an average method for estimating the reduction of the Heat Loss Coefficient of an energetically retrofitted occupied office building

Irati Uriarte[1], Aitor Erkoreka[1], Catalina Giraldo-Soto[1], Koldo Martin[1], Amaia Uriarte[2], Pablo Eguia[3]

[1]ENEDI Research Group, Department of Thermal Engineering, University of the Basque Country (UPV/EHU), Alda. Urquijo s/n, 48013 Bilbao, Spain.

Corresponding author e-mail: irati.uriarte@ehu.eus

[2] Tecnalia, Sustainable Construction Division, Parque Tecnológico de Bizkaia, C/Geldo, Edificio 700, 48160 Derio, Spain

[3]Department of Mechanical Engineering, Heat Engines and Fluid Mechanics, School of Industrial Engineering, University of Vigo, 36310 Vigo, Spain.

Abstract:

The performance gap between the design energy consumption of buildings and their real energy consumption has three main sources: the energy systems' performance, the users' behaviour and the buildings' envelope performance. The latter should be characterized under in-use conditions by estimating their in-use Heat Loss Coefficient (HLC). This work further develops an existing 'average method' by fully developing it from the energy conservation principle applied to a generic in-use building. Furthermore, the uncertainty sources are identified and limited through the mathematical development of the method. An innovative solution to the problematic of multizone buildings is also demonstrated, where HLC values should be calculated for different floors and then aggregated to obtain the entire building's HLC. Furthermore, all these can be done without the need of a detailed model of the building.

The improved average method has been applied to an occupied, energetically monitored office building of the University of the Basque Country. The building was energetically rehabilitated during the summer of 2017. Therefore, the proposed method has been applied over the three winters prior to rehabilitation and then, to the winter after the rehabilitation. It has thus been possible to estimate a 28% reduction of the HLC for the post-retrofitted case, as compared to the pre-retrofitted one.

Keywords: Building envelope energy performance, Heat Loss Coefficient (HLC), energy monitoring, average method.

Highlights:

- In-use energy characterization of the building envelope
- Analysis of the validity of the HLC estimation method
- Estimation of the HLC reduction in an energetically retrofitted office building

Declarations of interest: none

Abbreviations and units

- *ARMAX:* Autoregressive–moving-average models.
- *ARX:* Autoregressive with exogenous terms model.
- c_i: Specific heat of the ith incompressible material [kJ/kg K].
- cp_{air}: Constant pressure specific heat of the air at the average indoor temperature [kJ/kg K].
- C_v: Infiltration and/or ventilation heat loss coefficient [kW/K].
- $C_{v(vent)}$: Ventilation heat loss coefficient [kW/K].
- $C_{v(inf)}$: Infiltration heat loss coefficient [kW/K].
- c_w: Specific heat of the water at the average flow and return temperatures [kJ/kg K].
- ΔT: Temperature difference [K].
- E_{cv}: Total energy of the system [kJ].
- $F_{i,j}$: The ith zone of the jth floor in a building.
- g: Gravity [m/s^2].
- *g-value:* Percentage of solar radiation incident in a window that is transmitted to the interior of the building [-].
- h: Enthalpy of the fluid in the inlet (subscript ‘i’) or in the exit (subscript ‘e’) of the system [kJ/kg].
- h_{ae}: Enthalpy of the returned air from the Control Volume [kJ/kg].
- h_{ai}: Enthalpy of the supplied air to the Control Volume [kJ/kg].
- *HLC (Heat Loss Coefficient):* Considers the building heat losses through envelope plus ventilation and/or infiltration per degree difference between indoor and outdoor temperatures. HLC = UA + C_v [kW/K].
- $HLC_{building}$: Heat Loss Coefficient calculated as a whole unique building.
- HLC_{simple}: Heat Loss Coefficient calculated without considering the solar gains.
- HLC_{sum}: Heat Loss Coefficient calculated as the sum of each individual floor HLC.
- H_{sol}: Horizontal global solar radiation [kW/m^2].
- *HVAC:* Heating, ventilation, and air conditioning technology.
- h_{we}: Enthalpy of the returned water from Control Volume [kJ/kg].
- h_{wi}: Enthalpy of the supplied water to the Control Volume [kJ/kg].
- K: All the other heat gains inside the building excluding solar gains ($S_a \cdot V_{sol}$) and all heating system gains (Q) [kW]. $K = K_{electricity} + K_{occupancy}$.
- *KE:* Kinetic energy of the system [kJ]. The energy of an object owing to its movement.
- $K_{electricity}$: Heat gains inside the building due to electricity consumed within the building envelope [kW].
- $K_{occupancy}$: Heat gains inside the building due to metabolic generation of the occupants [kW].
- *KPI:* Key Performance Indicator, in this work referring to HLC, $S_a \cdot V_{sol}$, UA and C_v.
- m_i: The different mass types within the building [kg].
- $\dot{m}$: Mass flow rate of the fluid in the inlet (subscript ‘i’) or in the exit (subscript ‘e’) of the system [kg/s].
- $\dot{m}_{air}$: Air mass flow rate [kg/s].
- $\dot{m}_{water}$: Water mass flow rate within the heating system circuit [kg/s].
- η: Heat recovery system efficiency.
- *PE:* Potential energy of the system [kJ]. There are several types of potential energy. In this work we refer to the gravitational potential energy.

- P_{in}: Pressure inside the building [bar].
- P_{out}: Pressure outside the building [bar].
- $\dot{Q}_{cv}$: The heat exchanged through the Control Volume [kW].
- Q or $Q_{heating}$: All heating systems' energy inputs inside the building [kW].
- $Q_{infiltration}$: Heat losses of the building due to infiltrations [kW].
- $Q_{inf+vent}$: Sum of $Q_{infiltration}$ and $Q_{ventilation}$ [kW].
- $Q_{recovery}$: Heat exchanged between flow and return streams in a ventilation system's heat recovery system [kW].
- $Q_{transmission}$: Heat losses of the building due to transmission losses [kW].
- $Q_{ventilation}$: Heat losses of the building due to ventilation system [kW].
- ρ_{air}: Density of the air at the average indoor temperature [kg/m^3].
- S_a *(solar aperture):* Equivalent southern, vertical, perfectly transparent surface that allows the same solar energy as to the whole building to enter referred to the south vertical global solar radiation [m^2].
- *t:* time, any variable with a '(t)' is a time dependant variable [s].
- t_1: Time period's first hour [h].
- t_N: Time period's last hour [h].
- T_{exh}: Temperature of the exhausted air after crossing the heat recovery system [K or ºC].
- $T_{Fi,j}$: Specific temperature of the ith zone of the jth floor [K or ºC].
- T_G: Ground temperature [K or ºC].
- T_{in}: Indoor air temperature [K or ºC].
- T_{out}: Outdoor air temperature [K or ºC].
- T_{sup}: Temperature of the supply air after crossing the heat recovery system [K or ºC].
- T_w: Temperature of the water in the inlet (subscript 'i') or in the exit (subscript 'e') of the system [K or ºC].
- *U:* Internal energy of the system [kJ]. It considers the energy gains and losses inside the system as a result of the changes that take place in the internal state.
- *UA:* Considered building envelope transmission heat transfer coefficient [kW/K].
- *v:* Velocity of the fluid in the inlet (subscript 'i') or in the exit (subscript 'e') of the system [m/s].
- $\dot{V}_{air}$: Volumetric air flow rate [m^3/s].
- $\dot{V}_{air(vent)}$: Ventilation volumetric air flow rate [m^3/s].
- $\dot{V}_{air(inf)}$: Infiltration volumetric air flow rate [m^3/s].
- V_{sol}: South vertical global solar radiation [kW/m^2].
- $\dot{W}_{cv}$: The work exchanged through the Control Volume [kW].
- *z:* Elevation of the fluid in the inlet (subscript 'i') or in the exit (subscript 'e') of the system [m].

1. Introduction

The European Union commitment to energy efficiency can be clearly seen in the directives and objectives proposed for the years 2020, 2030 and 2050 [1]. Energy saving and energy efficiency when constructing or rehabilitating a building is one of the main aims. According to H2020 Energy Efficient Buildings (EeB) [2], buildings are responsible for 40% of energy consumption and 36% of CO_2 emissions in the EU. The first thermal regulation was introduced in Europe in the 1970s [3]. Since millions of buildings in Europe were constructed before then, in general, energy efficiency was not considered a main issue in any of those buildings [3, 4].

Several countries in the European Union have developed different energy performance estimation methods, where they use whole building simulation software with thermal models [5]. However, Summerfield [6] established that energy saving methods should be based on empirical methods instead of model estimations. Moreover, in general, these models assume standard operation conditions and consequently, the occupation and real heat requirements are not considered in these simulations. Therefore, unless fed with monitored occupation and HVAC system data, simulation models tend to overestimate the energy demand of old buildings and to underestimate it in new buildings [6].

On the other hand, advanced mathematical modelling techniques, such as ARMAX [7, 8] (ARX) and Grey Box modelling (state space models) [9-11], have been used by different authors to identify the real energy behaviour of building envelopes or building components based on measurements [12]. Some of those methods even identify such building characteristics as U values, thermal resistances, thermal capacitances and solar apertures. Due to the limitations of installing sensors in in-use buildings, the advanced mathematical modelling techniques, where physical–statistical approaches are used, have become common [13].

When working with state space models, it is important to obtain some previous physical knowledge of the building. The analysis consists of fitting several models, starting from the simplest and going on to the most complex, comparing their log likelihood values and residuals. Therefore, it is very important to obtain accurate results on the diffusion term in order to verify the quality of the model [11, 12]. On the other hand, when working with ARMAX models, single and multi-output models [7, 8] can be developed. Comparing with the state space equation, the ARMAX models do not need previous physical knowledge. Unfortunately, since the ARMAX models do not identify steady state physical parameters, the results obtained are estimated by comparing the ARMAX model and the steady state energy balance equation [12].

Here, an important "performance gap" [14] is observed when designed or simulated energy consumptions are compared to real ones. Apart from the simulation error, there are such parameters as occupancy [15, 16], weather data [17], material uncertainty [18], etc., which are difficult to model accurately. Although the "performance gap" can be affected by the user behaviour and the buildings' systems real energy performance [19], the building envelope also has a considerable influence on it. The most commonly used Key Performance Indicators (KPI) for the building envelope energy performance characterization are the Heat Loss Coefficient (HLC [kW/K], which considers transmission heat losses through the envelope (UA [kW/K]), plus ventilation and/or infiltration heat losses (C_v [kW/K])) and the solar gains, usually given on a daily basis in [kW/day] [20].

Although there are some research works that estimate these Key Performance Indicators in monitored in-use buildings [21], it is still far from being a general method. Of the existing methods to estimate the building envelope Heat Loss Coefficient, the Co-heating method is the most developed, and it also includes specific testing procedures [20, 22, 23]. However, it is not prepared for working with in-use buildings, due to the difficulties when estimating such parameters as solar gains or occupancy [24, 25].

In this work, the average method presented in [26] to estimate the HLC of an in-use building is further developed. As a main novelty, in this paper, the whole mathematical demonstration, starting from the energy conservation equation, is developed in order to enable comprehension of the limits the method has when applied to in-use buildings. Thus, the period selection criteria for reliable HLC estimation by the average method has been defined in detail, for minimizing the HLC estimate uncertainty.

This method does not require to build a detailed physical model of the building to estimate its in-use HLC. Thus, it could be used within Building Management System's programing in a general way, with the only need to be fed by the total window area of the building, the scheduled occupancy data and the already widespread energy monitoring data. The paper also focuses on the innovative demonstration of the summation properties of the HLC values when estimated floor by floor. Therefore, a multizone building is presented and the detailed heat and mass exchanges between the zones or volumes and adjacent surroundings are analysed to prove the HLC summation properties. Note that the reliable in-use HLC estimation should be achievable by analysing the data sets obtained by already widespread building monitoring systems simply made up of indoor and outdoor temperatures, heating system energy inputs to the building, electricity consumption and weather data.

Finally, the paper studies the pre- and post-retrofitting HLC values of an in-use office building. Therefore, the calculations are presented into two sections: Analysis of the data before retrofitting (between November 2014 and March 2017) and analysis of the data after retrofitting (between November 2017 and March 2018). Then, a comparison is carried out between pre- and post-retrofitting in-use HLC values, where a drop in the HLC value is expected after the retrofitting.

2. Average method

2.1. Origin of the method

The origin of the method has been studied in detail in order to understand the method's limits when used in dynamic problems such as an in-use building. Figure 1 shows the system to be analysed from the Thermodynamics Open System viewpoint. As can be seen in Figure 1, the building's envelope is the Control Volume or the boundary of the system through which heat and mass can be exchanged with the surroundings and the ground. Eq. (1) states the energy conservation principle of a generic Thermodynamic Open System [27].

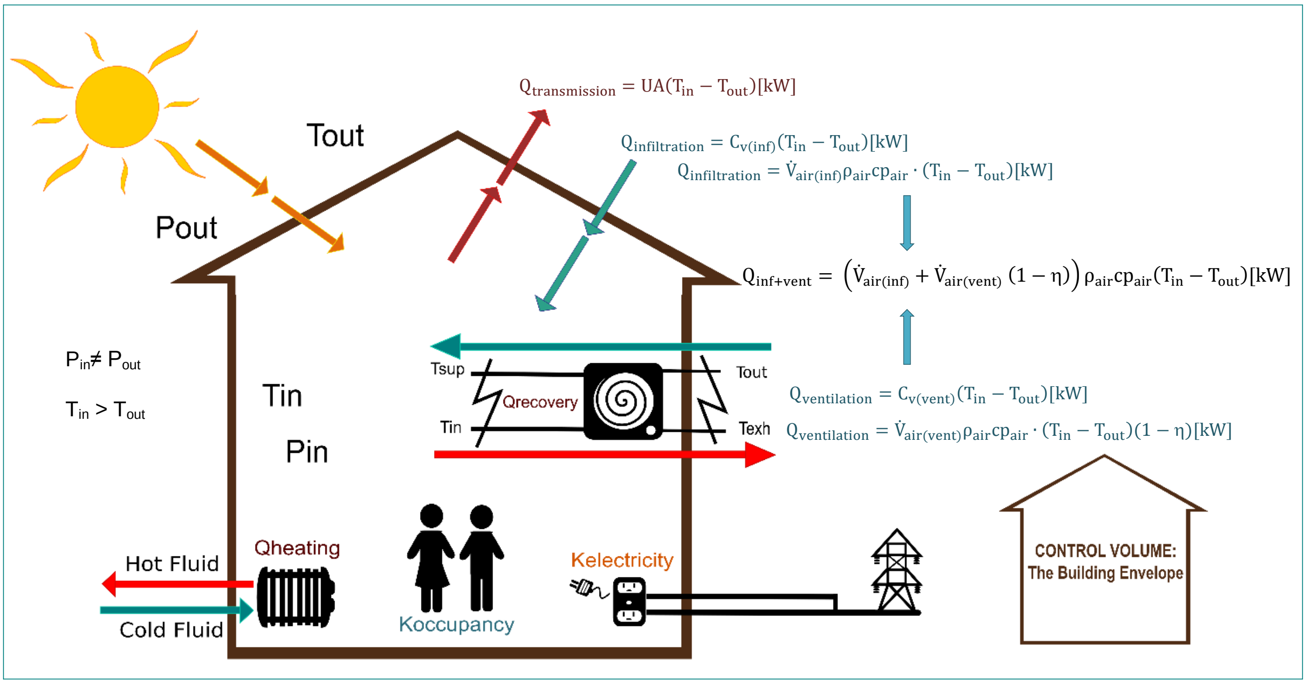

Figure 1. Schematic of all energy and mass exchanges through the control volume defined by the building envelope.

$$\left\{\begin{matrix}\text{Time rate of change}\\ \text{of the energy contained}\\ \text{within the control volume}\end{matrix}\right\} = \left\{\begin{matrix}\text{net rate at which energy}\\ \text{is being transferred in}\\ \text{by heat transfer at time t}\end{matrix}\right\} - \left\{\begin{matrix}\text{net rate at which energy}\\ \text{is being transferred out}\\ \text{by work transfer at time t}\end{matrix}\right\} + \left\{\begin{matrix}\text{net rate at which energy}\\ \text{transfer into the}\\ \text{control volume}\\ \text{accompanying mass flow}\end{matrix}\right\}$$

$$\frac{dE_{cv}}{dt} = \dot{Q}_{cv} - \dot{W}_{cv} + \sum_i \dot{m}_i\left(h_i + \frac{V_i^2}{2} + gz_i\right) - \sum_e \dot{m}_e\left(h_e + \frac{V_e^2}{2} + gz_e\right) \quad [kW] \qquad \text{Eq. (1)}$$

Each term of Eq. (1) is developed separately. So the first term represents the energy accumulation in the system, including the Internal Energy (U), the Kinetic Energy (KE) and the Potential Energy (PE). Since these last two terms are usually constant in a building, their derivative over time will be zero. Therefore, only the Internal Energy is relevant when estimating the energy accumulation term:

$$\frac{dE_{cv}}{dt} = \frac{dU}{dt} + \frac{dKE}{dt} + \frac{dPE}{dt} = \frac{dU}{dt} \qquad [kW] \qquad \text{Eq. (2)}$$

On the other hand, the second term in Eq. (1) takes into account all the pure heat exchanges occurring through the Control Volume boundary (the building envelope). In this case, the heat gained through the solar radiation entering the building and the metabolic heat generated by the occupants of the building are considered to be inputs. Nevertheless, the added negative inputs are transmission heat losses through the envelope of the building.

$$\dot{Q}_{CV} = S_a V_{sol} + K_{occupancy} - UA(T_{in} - T_{out}) \quad \text{[kW]} \qquad \text{Eq. (3)}$$

The next term, $\dot{W}_{cv}$, considers the pure work exchanged through the Control Volume. In this case, the consumed electricity is considered as work. However, as the electricity is converted into heat within the system, the considered negative work is presented as positive heat gain:

$$-\dot{W}_{CV} = K_{electricity} \quad \text{[kW]} \qquad \text{Eq. (4)}$$

Finally, the last two terms in Eq. (1) consider the net energy exchanged by the system due to the mass flow rates of the water (it could be other Heat Transfer Fluid) in the heating system and the air mass flow rates of the ventilation and/or infiltration air exchanges. Here, the heat provided by the heating system is considered in the energy balance equation as flow and return hot water of the heating system circuit (Eq. (5)). The hot water for the heating system could be produced by different technologies. If electrical heating is present, this would be considered in the Eq. (4) term.

If we have buildings without a ventilation system or a ventilation system without heat recovery, then the term $\dot{V}_{air(vent)}\rho_{air}cp_{air}(T_{in} - T_{out}) + \dot{V}_{air(\mathrm{inf})}\rho_{air}cp_{air}(T_{in} - T_{out})$ represents the heat exchanged by the building with the outdoor ambient due to both phenomena. If no ventilation system is present in the building, the ventilation term disappears. Then, the ventilation and/or infiltration heat losses can be calculated using the specific heat at constant pressure of the air, cp_{air}, and the indoor to outdoor temperatures (Eq. (5)). Kinetic and potential energy variations of both flows can be neglected.

$$\sum_i \dot{m}_i \left(h_i + \frac{V_i^2}{2} + gz_i\right) - \sum_e \dot{m}_e \left(h_e + \frac{V_e^2}{2} + gz_e\right) = \dot{m}_{water}(h_{wi} - h_{we}) + \dot{m}_{air}(h_{ai} - h_{ae}) =$$
$$\dot{m}_{water}c_w(T_{wi} - T_{we}) - \dot{V}_{air(vent)}\rho_{air}cp_{air}(T_{in} - T_{out}) - \dot{V}_{air(\mathrm{inf})}\rho_{air}cp_{air}(T_{in} - T_{out}) = \qquad \text{Eq. (5)}$$
$$\dot{m}_{water}c_w(T_{wi} - T_{we}) - Cv(T_{in} - T_{out}) = Q_{heating} - Q_{inf+vent} \quad \text{[kW]}$$

However, if the building is working on a ventilation system with heat recovery, the term $\dot{V}_{air(vent)}\rho_{air}cp_{air}(T_{in} - T_{out})$ of Eq. (5) should be calculated considering the heat recovery system efficiency. In order to check how the recovery system affects our calculations, it is necessary to develop the following equations. Figure 1 shows the schematic of the different temperatures involved in a generic heat recovery system for a ventilation system.

The heat recovery system works with four main temperatures: The outdoor or ambient temperature (T_{out}), the renewed or supply temperature (T_{sup}), the interior temperature (T_{in}) and the exhaust temperature (T_{exh}). The supplied and exhaust temperatures are those obtained after crossing the recovery system by both, the flow and return of the air flows. The supply temperature is that obtained after the external temperature crosses the recovery system. In winter, this temperature will increase. Considering an adiabatic heat exchanger and the same volumetric flow rates for supply and exhaust flows, the heat from the exhaust stream will be used to heat up the cold inlet stream. Thus, the temperature drop of the exhaust stream should be equal to the inlet stream temperature increase across the heat exchanger. Therefore, the percentage of heat recovered would be defined as in Eq. (6):

$$\eta = \frac{T_{sup} - T_{out}}{T_{in} - T_{out}} \qquad \text{Eq. (6)}$$

Eq. (7) represents the heat exchanged inside the heat exchanger, while Eq. (8) represents the heat that the ventilation system will require for the building's heating system.

$$Q_{recovery} = \dot{V}_{air(vent)}\rho_{air}cp_{air} \cdot (T_{in} - T_{exh}) = \dot{V}_{air(vent)}\rho_{air}cp_{air} \cdot (T_{sup} - T_{out}) \text{ [kW]} \qquad \text{Eq. (7)}$$

$$Q_{ventilation} = \dot{V}_{air(vent)}\rho_{air}cp_{air} \cdot (T_{in} - T_{sup}) \text{ [kW]} \qquad \text{Eq. (8)}$$

Developing Eq. (6), a relation between T_{sup}, T_{in}, T_{out} and η can be obtained. Then, combining Eq. (8) and Eq. (9), Eq. (10) would be obtain.

$$T_{sup} = (1 - \eta) \cdot T_{out} + \eta \cdot T_{in} \text{ [ºC]} \qquad \text{Eq. (9)}$$

$$Q_{ventilation} = \dot{V}_{air(vent)}\rho_{air}cp_{air}((1 - \eta) \cdot T_{out} + \eta \cdot T_{in} - T_{out}) \text{ [kW]} \qquad \text{Eq. (10)}$$

Then, $Q_{ventilation}$ can also be presented as:

$$Q_{ventilation} = \dot{V}_{air(vent)}\rho_{air}cp_{air}(1 - \eta)(T_{in} - T_{out}) \text{ [kW]} \qquad \text{Eq. (11)}$$

Therefore, if the heat recovery system is added to the building, the previously presented Eq. (5) is converted into Eq. (13), where:

$$C_v = \dot{V}_{air(vent)}\rho_{air}cp_{air} \cdot (1 - \eta) + \dot{V}_{air(\text{inf})}\rho_{air}cp_{air} \qquad \text{[kW/K]} \qquad \text{Eq. (12)}$$

$$\sum_i \dot{m}_i \left(h_i + \frac{V_i^2}{2} + gz_i\right) - \sum_e \dot{m}_e \left(h_e + \frac{V_e^2}{2} + gz_e\right) = \dot{m}_{water}(h_{wi} - h_{we}) + \dot{m}_{air}(h_{ai} - h_{ae})\eta =$$

$$\dot{m}_{water} c_w (T_{wi} - T_{we}) - \dot{V}_{air(vent)} \rho_{air} cp_{air} (T_{in} - T_{out})(1 - \eta) - \dot{V}_{air(\text{inf})} \rho_{air} cp_{air} (T_{in} - T_{out}) = \quad \text{Eq. (13)}$$

$$\dot{m}_{water} c_w (T_{wi} - T_{we}) - Cv\,(T_{in} - T_{out}) = Q_{heating} - Q_{inf+vent} \ \text{[kW]}$$

If we put together all the terms developed in Eq. (1), we then obtain the Eq. (14) expression for the complete energy balance of the building at the time instant t. In this paper, the heat losses to the ground have been considered within the HLC value, as if they were working against ($T_{in} - T_{out}$). Note that the long wave radiative heat exchange occurring in the building envelope is again considered within the HLC value, as if they were working against ($T_{in} - T_{out}$). These last two assumptions are also made in the original Co-heating method [20], where the UA and C_v values are also considered to be constant.

$$\frac{dU(t)}{dt} = S_a V_{sol}(t) + K_{occupancy}(t) - UA(T_{in} - T_{out})(t) + K_{electricity}(t) + Q_{heating}(t) -$$

$$Cv\,(T_{in} - T_{out})(t) \ \text{[kW]} \quad \text{Eq. (14)}$$

$$\frac{dU(t)}{dt} = S_a V_{sol}(t) + Q_{heating}(t) + K_{electricity}(t) + K_{occupancy}(t) - (UA + Cv)(T_{in} - T_{out})(t) \ \text{[kW]}$$

If C_v is defined as in Eq. (5) or as in Eq. (13), then Eq. (14) is valid for any type of ventilation system of a building and the HLC can be estimated by:

$$HLC = (UA + C_v) \ \text{[kW/K]} \quad \text{Eq. (15)}$$

$$\frac{dU(t)}{dt} = S_a V_{sol}(t) + Q_{heating}(t) + K_{electricity}(t) + K_{occupancy}(t) - HLC(T_{in} - T_{out})(t) \ \text{[kW]} \quad \text{Eq. (16)}$$

Analysing Eq. (16), it could be said that if the building's HLC is to be estimated by means of measurements, it would be necessary to make an instantaneous measurement of the energy rate being stored in the building $\left(\frac{dU(t)}{dt}\right)$, the exact solar gains at the same instant $\left(S_a \cdot V_{sol}(t)\right)$, the exact instantaneous heating gains $\left(Q_{heating}(t)\right)$, the exact instantaneous internal gains due to occupants and electricity consumption $(K_{electricity}(t) + K_{occupancy}(t))$ and the exact indoor to outdoor temperature difference $(T_{in} - T_{out})(t)$. Obviously, the instantaneous accumulation term is nearly impossible to measure accurately and the exact instantaneous solar gains are also difficult to measure in an in-use building. The rest of the terms can be measured accurately and instantaneously.

If $Q(t) = Q_{heating}(t)$ and $K(t)$ in Eq. (17), then reordering Eq. (16), we obtain the Eq. (18):

$$K(t) = K_{electricity}(t) + K_{occupancy}(t) \quad \text{[kW]} \qquad \text{Eq. (17)}$$

$$-\frac{dU(t)}{dt} + Q(t) + K(t) = HLC(T_{in} - T_{out})(t) - S_a V_{sol}(t) \quad \text{[kW]} \qquad \text{Eq. (18)}$$

Since the internal energy is a property of the system and we consider the HLC to be constant, making the integer over a period of time considered between t_1 and t_N, we can convert Eq. (18) into:

$$-\int_{u_1}^{u_N} dU(t) + \int_{t_1}^{t_N} Q(t)dt + \int_{t_1}^{t_N} K(t)dt = HLC\int_{t_1}^{t_N}(T_{in} - T_{out})(t)dt - \int_{t_1}^{t_N} S_a V_{sol}(t)dt \quad \text{[kJ]}$$

$$-\sum_{i=1}^{z} m_i(u_i(t_N) - u_i(t_1)) + \int_{t_1}^{t_N} Q(t)dt + \int_{t_1}^{t_N} K(t)dt = HLC\int_{t_1}^{t_N}(T_{in} - T_{out})(t)dt - \int_{t_1}^{t_N} S_a V_{sol}(t)dt \quad \text{[kJ]} \qquad \text{Eq. (19)}$$

$$\sum_{i=1}^{z} m_i c_i(T_i(t_1) - T_i(t_N)) + \int_{t_1}^{t_N} Q(t)dt + \int_{t_1}^{t_N} K(t)dt = HLC\int_{t_1}^{t_N}(T_{in} - T_{out})(t)dt - \int_{t_1}^{t_N} S_a V_{sol}(t)dt \quad \text{[kJ]}$$

where m_i are the different mass types within the building (the analysed system), such as concrete, bricks, furniture, wood (the sum goes up to z different types of masses present within the building), which might change their temperatures (and thus their internal energy) when going from time instant t_1 to t_N. The c_i represents the different specific heats of the different masses within the system. For the air within the building, the specific heat at constant volume should be used. Since monitoring systems make discrete measurements every Δt, the integers of Eq. (19), would be converted into sums from k =1 (at t_1) to k = N (at t_N):

$$\sum_{i=1}^{z} m_i c_i(T_i(t_1) - T_i(t_N)) + \sum_{k=1}^{N} Q_k \Delta t + \sum_{k=1}^{N} K_k \Delta t = HLC\sum_{k=1}^{N}(T_{in,k} - T_{out,k})\Delta t - \sum_{k=1}^{N}(S_a V_{sol})_k \Delta t \quad \text{[kJ]} \qquad \text{Eq. (20)}$$

Thus, if the thermal level is not equal at the start and end of the analysis period from Eq. (20), we could solve for HLC as in Eq. (21). Note that Δt cannot be cancelled because the thermal storage is a property that depends solely on the initial and final thermal level of the building and not on the time dependant path as are the rest of the variables of the equation:

$$HLC = \frac{\sum_{i=1}^{z} m_i c_i(T_i(t_1) - T_i(t_N)) + \sum_{k=1}^{N}(Q_k + K_k + (S_a V_{sol})_k)\Delta t}{\sum_{k=1}^{N}(T_{in,k} - T_{out,k})\Delta t} \quad \text{[kW/K]} \qquad \text{Eq. (21)}$$

In Eq. (21), it can be seen that the longer the considered period is, the smaller the impact of the difference in thermal level of the building on the HLC estimate. Since the internal energy of the building is a property, it only depends on the initial and final states of the building. While the denominator increases, the longer the period is. The accumulation term is very hard to estimate accurately. The proposed average method is formed by selected periods, where the initial indoor and outdoor temperatures (at t_1) and final indoor and outdoor temperatures (at t_N) are equal. In other words, both indoor and outdoor temperatures must be equal at the start and end of the periods. Thus, the average temperature between the indoor and outdoor temperature will also be equal at t_1 and t_N. If this is fulfilled, it can be assumed that there will be no accumulated heat in the building, since the start and end points of the analysed period will have the same thermal level. Then, the energy accumulation inside the building will be negligible between these two time instants and it will be possible to ensure similar conditions as in the stationary stage for the selected period. Since the longer the period is, the smaller the impact of the accumulation term, as proved in Eq. (21); if the period fulfils the same initial and final thermal level conditions, applying the method to periods of at least 72 hours (three days), the accumulation term effect on the HLC, by Eq. (25), will be negligible. Therefore, if it can be assumed that $T(t_1) = T(t_N)$ for a period, then Eq. (19) can be rewritten as:

$$\sum_{i=1}^{z} m_i c_i(0) + \int_{t_1}^{t_N} Q(t)dt + \int_{t_1}^{t_N} K(t)dt = HLC \int_{t_1}^{t_N} (T_{in} - T_{out})(t)dt - \int_{t_1}^{t_N} S_a V_{sol}(t)dt \quad \text{[kJ]}$$

$$\int_{t_1}^{t_N} Q(t)dt + \int_{t_1}^{t_N} K(t)dt = HLC \int_{t_1}^{t_N} (T_{in} - T_{out})(t)dt - \int_{t_1}^{t_N} S_a V_{sol}(t)dt \quad \text{[kJ]} \qquad \text{Eq. (22)}$$

Since monitoring systems make discrete measurements every Δt, the integers of Eq. (22) would be converted into sums from k =1 (at t_1) to k = N (at t_N):

$$\sum_{k=1}^{N} Q_k \Delta t + \sum_{k=1}^{N} K_k \Delta t = HLC \sum_{k=1}^{N} (T_{in,k} - T_{out,k}) \Delta t - \sum_{k=1}^{N} (S_a V_{sol})_k \Delta t \quad \text{[kJ]} \qquad \text{Eq. (23)}$$

Taking Δt as a common factor and cancelling it:

$$\sum_{k=1}^{N} Q_k + \sum_{k=1}^{N} K_k = HLC \sum_{k=1}^{N} (T_{in,k} - T_{out,k}) - \sum_{k=1}^{N} (S_a V_{sol})_k \quad \text{[kW]} \qquad \text{Eq. (24)}$$

and, finally, reordering Eq. (24), we obtain Eq. (25):

$$HLC = \frac{\sum_{k=1}^{N}(Q_k+K_k+(S_aV_{sol})_k)}{\sum_{k=1}^{N}(T_{in,k}-T_{out,k})} \quad \text{[kW/K]} \qquad \text{Eq. (25)}$$

The second term introducing uncertainties in the method application are the solar gains of Eq. (25). The method proposes using periods, not only with the same initial and final temperature of the building, but also with cold and cloudy periods where solar radiation is very low and could thus be considered purely diffuse [28]. For cloudy periods, where the radiation can be considered purely diffuse, any orientation global radiation measurement can be used since any of these measurements will be similar to a diffuse solar radiation measurement. These periods can be easily found in countries or areas where cloudy and cold days are common in winter. It must be possible to ensure that the solar heat gains for those periods compared to the rest of the heat gains (heating (Q) + all internal gains excluding solar radiation (K)) of the building are less than 10%. Then, if these roughly estimated solar gains have an uncertainty as large as 100%, their effect on the HLC estimation would only be 10%. Accurately measuring heating and internal gains is possible, while measuring solar gains accurately is a hard task. However, if only cloudy days are present in the studied period and it can be considered that only diffuse solar radiation is affecting the whole building envelope, then it is possible to make a rough estimate of the solar gains.

To make a rough estimate of the solar gains, it can be considered that multiplying the total window area of the building envelope by a g-value of 0.5 [29], a rough estimation of the solar aperture regarding the diffuse radiation can be obtained. Since diffuse radiation can be considered to be similar in all orientations, if this value is multiplied by the solar aperture, the internal gains created by the solar radiation can be estimated. Therefore, it is reasonably easy to make rough estimates of the (S_aV_{sol}) term in cloudy periods. Hence, due to the similarity between the results of S_aV_{sol} and S_aH_{sol} in cloudy periods, the method could be applied using any of them indistinctly.

If the period is also cold, the weight of the solar gains in the energy balance is small and enables us to make accurate estimates of the HLC, even though the solar gains are roughly calculated. This work considers a period to be cold if the average indoor to outdoor temperature difference is 10ºC or bigger.

Thus, the uncertainty associated with the indoor to outdoor temperature difference is limited. For example, a 0.5ºC uncertainty in the indoor to outdoor temperature difference will only represent a 5% error in the indoor to outdoor temperature difference. Furthermore, the method also proposes calculating the HLC, assuming the $(S_a V_{sol})$ term to be zero, as shown in Eq. (26). Thus, the effect of the solar gains of the period on the HLC can be analysed.

$$HLC_{simple} = \frac{\sum_{k=1}^{N}(Q_k + K_k)}{\sum_{k=1}^{N}(T_{in,k} - T_{out,k})} \quad \text{[kW/K]} \qquad \text{Eq. (26)}$$

Eq. (26) introduces errors up to 10-15% in the estimated HLCs in the considered periods of very low solar radiation, as compared to Eq. (25). However, Eq. (26), although slightly underestimated, makes it simple to obtain quite a reliable HLC value of a building. From now on, the HLC of Eq. (25) will be named HLC, while the HLC of Eq. (26) will be named HLC_{simple}.

This proposed average method has some similar characteristics regarding the mathematical estimation method used by the ISO 9869-1 method [30] for obtaining in-situ U-values of walls. The method described by the ISO 9869-1 requires plotting the accumulated average U-value during the periods considered valid for the estimation. On those plots, a stabilization band of ± 2% of the final estimate during the last 24 hours of the testing period is required. Based on the mathematical development carried out in this paper for the whole building in-use HLC estimation method, due to the complexity of a whole building when compared to a single wall analysis and considering the uncertainty limits imposed, this band will be expanded to ± 10%. In other words, the proposed average method will also perform the HLC accumulated average plots for the selected periods and should be able to provide stable HLC values within a $\pm 10\%$ during the last 24 hours in order to ensure a reliable HLC estimation (see Appendix B examples).

2.2. Application to a multizone building

In this section, the properties of the HLC estimation related to a multizone building are analysed. As shown in Section 2.1, several heat gains and losses have been considered when estimating the Heat Loss Coefficient for a whole building enclosed in a control volume. However, the demonstration only considers the HLC estimation for a whole building with homogeneous indoor temperature. Section 2.2 explains how different rooms next to each other, or on different storeys located above or under each other, behave when considering the whole building HLC. It is proved how the internal heat and mass transfer effects passing from one room to another can be cancelled out through the following simple case:

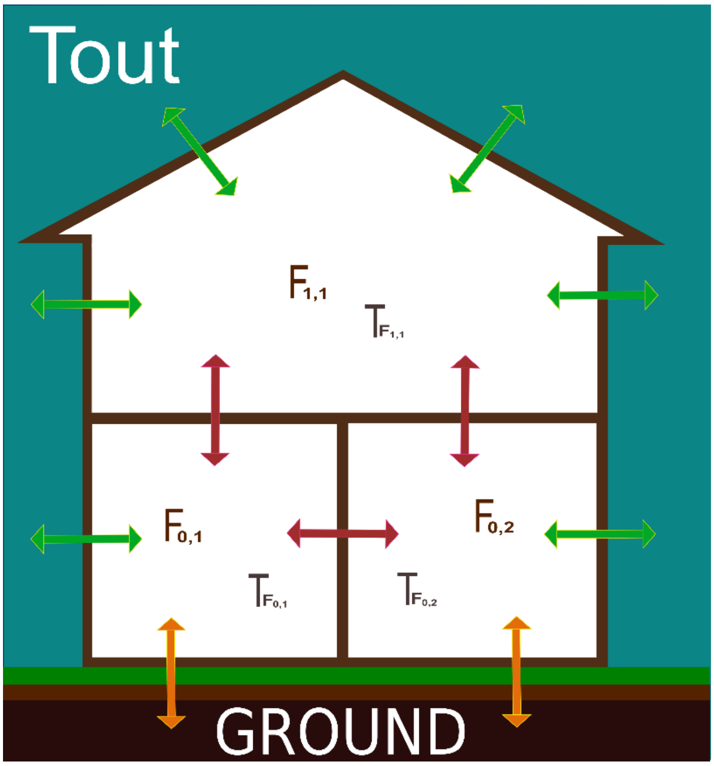

Figure 2. Schematic of all heat and mass exchanges through the multizone building.

Figure 2 shows the proposed simple case for a multizone building. Three different zones, distributed on two floors (F0 and F1), form the building. Each zone is affected by different heat and mass exchanges, coming either from other zones, the ground or the exterior. Thus, we aim to prove that for a building with L floors and M zones per floor, the building's total Heat Loss Coefficient can be estimated by applying the following formula:

$$HLC_{sum} = \sum_{i=1}^{L} \sum_{j=1}^{M} HLC_{Fi,j} \qquad \text{Eq. (27)}$$

$$HLC_{sum} = HLC_{F0,1} + HLC_{F0,2} + HLC_{F1,1} \quad \text{[kW/K]} \qquad \text{Eq. (28)}$$

where each zone HLC can be estimated by applying Eq. (25) directly to each zone as if they were only affected by $\left(T_{Fi,j} - T_{out}\right)$. For clarity, the sum from k = 1 to k = N is not shown in this section developments. The sum is only presented in the generalized equations Eq. (41) and Eq. (46).

$$HLC_{F0,1} = \frac{[Q_{F0,1}+K_{F0,1}+(S_a V_{sol})_{F0,1}]}{(T_{F0,1}-T_{out})} \text{ [kW/K]} \quad \text{Eq. (29)}$$

$$HLC_{F0,2} = \frac{[Q_{F0,2}+K_{F0,2}+(S_a V_{sol})_{F0,2}]}{(T_{F0,2}-T_{out})} \text{ [kW/K]} \quad \text{Eq. (30)}$$

$$HLC_{F1,1} = \frac{[Q_{F1,1}+K_{F1,1}+(S_a V_{sol})_{F1,1}]}{(T_{F1,1}-T_{out})} \text{ [kW/K]} \quad \text{Eq. (31)}$$

In this example, two zones are on the ground floor and another one on the first floor. Thus, the whole energy balance of each zone (Eq. (32) to Eq. (34)) is presented considering all transmission and infiltration exchanges for each of them:

Ground floor (zone F0,1):

$$Q_{F0,1} + K_{F0,1} + (S_a V_{sol})_{F0,1} = UA_{F0,1-G}\left(T_{F0,1} - T_G\right) + UA_{F0,1-F0,2}\left(T_{F0,1} - T_{F0,2}\right) + UA_{F0,1-F1,1}\left(T_{F0,1} - T_{F1,1}\right) + UA_{F0,1-out}\left(T_{F0,1} - T_{out}\right) + \dot{V}_{F0,1-F0,2}\rho_{air}cp_{air}\left(T_{F0,1} - T_{F0,2}\right) + \dot{V}_{F0,1-F1,1}\rho_{air}cp_{air}\left(T_{F0,1} - T_{F1,1}\right) + C_{v\,F0,1-out}\left(T_{F0,1} - T_{out}\right) \quad \text{[kW]} \quad \text{Eq. (32)}$$

Ground floor (zone F0,2):

$$Q_{F0,2} + K_{F0,2} + (S_a V_{sol})_{F0,2} = UA_{F0,2-G}\left(T_{F0,2} - T_G\right) + UA_{F0,2-F0,1}\left(T_{F0,2} - T_{F0,1}\right) + UA_{F0,2-F1,1}\left(T_{F0,2} - T_{F1,1}\right) + UA_{F0,2-out}\left(T_{F0,2} - T_{out}\right) + \dot{V}_{F0,2-F0,1}\rho_{air}cp_{air}\left(T_{F0,2} - T_{F0,1}\right) + \dot{V}_{F0,2-F1,1}\rho_{air}cp_{air}\left(T_{F0,2} - T_{F1,1}\right) + C_{v\,F0,2-out}\left(T_{F0,2} - T_{out}\right) \quad \text{[kW]} \quad \text{Eq. (33)}$$

First floor (zone F1,1):

$$Q_{F1,1} + K_{F1,1} + (S_a V_{sol})_{F1,1} = UA_{F1,1-F0,2}\left(T_{F1,1} - T_{F0,2}\right) + UA_{F1,1-F0,1}\left(T_{F1,1} - T_{F0,1}\right) + UA_{F1,1-out}\left(T_{F1,1} - T_{out}\right) + \dot{V}_{F1,1-F0,2}\rho_{air}cp_{air}\left(T_{F1,1} - T_{F0,2}\right) + \dot{V}_{F1,1-F0,1}\rho_{air}cp_{air}\left(T_{F1,1} - T_{F0,1}\right) + C_{v\,F1,1-out}\left(T_{F1,1} - T_{out}\right) \quad \text{[kW]} \quad \text{Eq. (34)}$$

When Eq. (32) to Eq. (34) are summed, the energy transfers through internal walls due to transmission and infiltration between the considered zones are cancelled out. Then, only heat and mass transfers between indoor and outdoor air and heat transfer between floor 0 zones and ground remain.

$$[Q_{F0,1} + K_{F0,1} + (S_aV_{sol})_{F0,1}] + [Q_{F0,2} + K_{F0,2} + (S_aV_{sol})_{F0,2}] + [Q_{F1,1} + K_{F1,1} + (S_aV_{sol})_{F1,1}] = UA_{F0,1-G}(T_{F0,1} - T_G) + UA_{F0,1-out}(T_{F0,1} - T_{out}) + C_{v\,F0,1-out}(T_{F0,1} - T_{out}) + UA_{F0,2-G}(T_{F0,2} - T_G) + UA_{F0,2-out}(T_{F0,2} - T_{out}) + C_{v\,F0,2-out}(T_{F0,2} - T_{out}) + UA_{F1,1-out}(T_{F1,1} - T_{out}) + C_{v\,F1,1-out}(T_{F1,1} - T_{out}) \quad \text{[kW]} \qquad \text{Eq. (35)}$$

Taking $\left(T_{F_{i,j}} - T_{out}\right)$ as the common factor for each zone:

$$[Q_{F0,1} + K_{F0,1} + (S_aV_{sol})_{F0,1}] + [Q_{F0,2} + K_{F0,2} + (S_aV_{sol})_{F0,2}] + [Q_{F1,1} + K_{F1,1} + (S_aV_{sol})_{F1,1}] = \left(UA_{F0,1-G}\frac{(T_{F0,1}-T_G)}{(T_{F0,1}-T_{out})} + UA_{F0,1-out} + C_{v\,F0,1-out}\right)(T_{F0,1} - T_{out}) + \left(UA_{F0,2-G}\frac{(T_{F0,2}-T_G)}{(T_{F0,2}-T_{out})} + UA_{F0,2-out} + C_{v\,F0,2-out}\right)(T_{F0,2} - T_{out}) + \left(UA_{F1,1-out} + C_{v\,F1,1-out}\right)(T_{F1,1} - T_{out}) \quad \text{[kW]} \qquad \text{Eq. (36)}$$

and, reordering Eq. (36), we obtain Eq. (37):

$$[Q_{F0,1} + K_{F0,1} + (S_aV_{sol})_{F0,1}] + [Q_{F0,2} + K_{F0,2} + (S_aV_{sol})_{F0,2}] + [Q_{F1,1} + K_{F1,1} + (S_aV_{sol})_{F1,1}] = HLC_{F0,1}(T_{F0,1} - T_{out}) + HLC_{F0,2}(T_{F0,2} - T_{out}) + HLC_{F1,1}(T_{F1,1} - T_{out}) \quad \text{[kW]} \qquad \text{Eq. (37)}$$

Eq. (37) proves that the only valid solution for any $T_{Fi,j}$ is the one provided by Eq. (29) to Eq. (31) for each of the $HLC_{Fi,j}$ of Eq. (37), where each $HLC_{Fi,j}$ has only the indoor to outdoor UA and C_v values within it. Remember that the $HLC_{F0,j}$ of the ground floor also includes the UA value against the ground multiplied by the factor $\frac{(T_{F0,j}-T_G)}{(T_{F0,j}-T_{out})}$.

Thus, it has been proven that the whole building Heat Loss Coefficient can be estimated by the sum of the individual zones $HLC_{Fi,j}$ as if they were only exchanging heat and mass with the outdoor air:

$$HLC_{sum} = \frac{[Q_{F0,1}+K_{F0,1}+(S_aV_{sol})_{F0,1}]}{(T_{F0,1}-T_{out})} + \frac{[Q_{F0,2}+K_{F0,2}+(S_aV_{sol})_{F0,2}]}{(T_{F0,2}-T_{out})} + \frac{[Q_{F1,1}+K_{F1,1}+(S_aV_{sol})_{F1,1}]}{(T_{F1,1}-T_{out})} = HLC_{F0,1} + HLC_{F0,2} + HLC_{F1,1} \quad \text{[kW/K]} \qquad \text{Eq. (38)}$$

Where the generic equation of each zone (or floor) can be presented as Eq. (39) for the simple HLC and Eq. (40) for the HLC:

$$HLC_{simple,F_{i,j}} = \frac{(Q_{F_{i,j}}+K_{F_{i,j}})}{(T_{F_{i,j}}-T_{out})} \quad \text{[kW/K]} \qquad \text{Eq. (39)}$$

$$HLC_{F_{i,j}} = \frac{(Q_{F_{i,j}} + K_{F_{i,j}} + (S_a V_{sol})_{F_{i,j}})}{(T_{F_{i,j}} - T_{out})} \quad \text{[kW/K]} \qquad \text{Eq. (40)}$$

Hence, generalizing the example to a building with L floors and M zones per floor, Eq. (38) can be written as Eq. (41). Considering Eq. (25) of Section 2.1, it can be written as the sum of N time step measurements for the period k =1 (at t_1) to k = N (at t_N):

$$HLC_{sum} = \sum_{i=1}^{L} \sum_{j=1}^{M} HLC_{Fi,j} = \sum_{i=1}^{L} \sum_{j=1}^{M} \sum_{k=1}^{N} \frac{(Q_{F_{i,j,k}} + K_{F_{i,j,k}} + (S_a V_{sol})_{F_{i,j,k}})}{(T_{F_{i,j,k}} - T_{out,k})} \quad \text{[kW/K]} \qquad \text{Eq. (41)}$$

From the previous analysis, it can be concluded that it is possible to develop a precise estimation of the whole building HLC estimating the Heat Loss Coefficients for each zone and summing them, since the transmissions and infiltration through the walls between the zones are cancelled out. Moreover, it must be commented that there is no physical meaning when measuring the HLCs of each zone independently, since this parameter does not consider the heat transmitted from one room to another. The individual HLC of each zone will only be physically meaningful when the same internal temperature is found in all the building's zones. Only there, each zone HLC will be representing the HLC regarding the indoor to outdoor exchange effects. For this specific case, where all $T_{Fi,j} = T_{in}$, then Eq. (38) becomes Eq. (42):

$$HLC_{sum} = \frac{[Q_{F0,1} + K_{F0,1} + (S_a V_{sol})_{F0,1}] + [Q_{F0,2} + K_{F0,2} + (S_a V_{sol})_{F0,2}] + [Q_{F1,1} + K_{F1,1} + (S_a V_{sol})_{F1,1}]}{(T_{in} - T_{out})} = HLC_{F0,1} + HLC_{F0,2} + HLC_{F1,1} \quad \text{[kW/K]} \qquad \text{Eq. (42)}$$

However, the proposed zone-by-zone development for the HLC estimation, as far as concerned, has not been used in order to estimate the HLC of a whole building. Instead of the HLC_{sum}, in previous works the $HLC_{building}$ has usually been estimated considering the whole building is a unique zone.

In order to estimate the $HLC_{building}$, Eq. (45) must be used, here, the sum of all the input parameters must be introduced (heating system's heat, occupancy and solar gains) for the whole building. Moreover, the internal temperature must be calculated as a unique indoor temperature. Usually two different methods are used: the average temperature method Eq. (43) and the volume weighted average temperature method Eq. (44).

$$T_{in} = \frac{T_{F0,1}+T_{F0,2}+T_{F1,1}}{3} \quad \text{[K or °C]} \qquad \text{Eq. (43)}$$

$$T_{in} = \frac{T_{F0,1}*V_{F0,1}+T_{F0,2}*V_{F0,2}+T_{F1,1}*V_{F1,1}}{V_{F0,1}+V_{F0,2}+V_{F1,1}} \quad \text{[K or °C]} \qquad \text{Eq. (44)}$$

Using the simple average temperature method, the formula in order to obtain the Figure 2 example building $HLC_{building}$ is the following:

$$HLC_{building} = \frac{[Q_{F0,1}+Q_{F0,2}+Q_{F1,1}]+[K_{F0,1}+K_{F0,2}+K_{F1,1}]+[(S_aV_{sol})_{F0,1}+(S_aV_{sol})_{F0,2}+(S_aV_{sol})_{F1,1}]}{\left(\frac{[T_{F0,1}+T_{F0,2}+T_{F1,1}]}{3}-T_{out}\right)} = \frac{[Q_{F0,1}+Q_{F0,2}+Q_{F1,1}]+[K_{F0,1}+K_{F0,2}+K_{F1,1}]+[(S_aV_{sol})_{F0,1}+(S_aV_{sol})_{F0,2}+(S_aV_{sol})_{F1,1}]}{(T_{in}-T_{out})} \quad \text{[kW/K]} \qquad \text{Eq. (45)}$$

Generalizing Eq. (45) to a building with L floors and M zones per floor, $HLC_{building}$ can be written as Eq. (46). Once again, considering Eq. (25) of Section 2.1, it can be written as the sum of N time step measurements for the period k =1 (at t_1) to k = N (at t_N):

$$HLC_{building} = \sum_{k=1}^{N} \frac{[\sum_{i=1}^{L}\sum_{j=1}^{M} Q_{i,j}+\sum_{i=1}^{L}\sum_{j=1}^{M} K_{i,j}+\sum_{i=1}^{L}\sum_{j=1}^{M}(S_aV_{sol})_{i,j}]_k}{(T_{in,k}-T_{out,k})} \quad \text{[kW/K]} \qquad \text{Eq. (46)}$$

The estimation of an average unique internal temperature can affect considerably the final $HLC_{building}$ estimation regarding the HLC_{sum} estimation value. Information is lost due to the internal temperature averaging process. Therefore, the Eq. (41) should provide more accurate results since each zone (or floor) has been analysed individually.

2.3. Error propagation

The existence of uncertainty due to measurements will be analysed in this section, since uncertainty sources due to modelling have already been detected and limited in Section 2.1. In this section, all uncertainties, excluding the one related to the accumulation term, are propagated to the estimation of the HLC. The effect of the accumulation term on the HLC estimate is assumed to be close to zero, considering the length of the period and the same thermal level condition to be established at the start and end of the valid data periods, as described in Section 2.1.

The error propagation method used in this section is based on the book [31]. The propagation of errors has been applied to the already presented Eq. (25) Heat Loss Coefficient formula, but using the period averaged values for all the variables:

$$HLC = \frac{\sum_{k=1}^{N}(Q_k+K_k+(S_aV_{sol})_k)}{\sum_{k=1}^{N}(T_{in,k}-T_{out,k})} = \frac{\frac{\sum_{k=1}^{N}(Q_k+K_k+(S_aV_{sol})_k)}{N}}{\frac{\sum_{k=1}^{N}(T_{in,k}-T_{out,k})}{N}} = \frac{\bar{Q}+\bar{K}+\overline{S_aV_{sol}}}{\overline{T_{in}}-\overline{T_{out}}} \quad \text{[kW/K]} \qquad \text{Eq. (47)}$$

The propagation of error for the addition and subtraction in Eq. (47) should be estimated first:

$$HLC = \frac{(\bar{Q}\pm\delta\bar{Q})+(\bar{K}\pm\delta\bar{K})+(\overline{S_aV_{sol}}\pm\delta\overline{S_aV_{sol}})}{(\overline{T_{in}}\pm\delta\overline{T_{in}})-(\overline{T_{out}}\pm\delta\overline{T_{out}})} = \frac{(\bar{Q}+\bar{K}+\overline{S_aV_{sol}})\pm(\delta\bar{Q}+\delta\bar{K}+\delta\overline{S_aV_{sol}})}{(\overline{T_{in}}-\overline{T_{out}})\pm(\delta\overline{T_{in}}+\delta\overline{T_{out}})} \quad \text{[kW/K]} \qquad \text{Eq. (48)}$$

In Eq. (48), all terms' uncertainties are considered, including that of the roughly estimated solar gains. Finally, the propagation error for the division in Eq. (48) must be calculated in order to estimate the error propagation when estimating the HLC of the building or of a zone within the building:

$$HLC = \frac{(\bar{Q}+\bar{K}+\overline{S_aV_{sol}})\pm(\delta\bar{Q}+\delta\bar{K}+\delta\overline{S_aV_{sol}})}{(\overline{T_{in}}-\overline{T_{out}})\pm(\delta\overline{T_{in}}+\delta\overline{T_{out}})}$$

$$= \frac{(\bar{Q}+\bar{K}+\overline{S_aV_{sol}})}{(\overline{T_{in}}-\overline{T_{out}})} \pm \left|\frac{(\bar{Q}+\bar{K}+\overline{S_aV_{sol}})}{(\overline{T_{in}}-\overline{T_{out}})}\right| \cdot \left(\frac{(\delta\bar{Q}+\delta\bar{K}+\delta\overline{S_aV_{sol}})}{|\bar{Q}+\bar{K}+\overline{S_aV_{sol}}|} + \frac{(\delta\overline{T_{in}}+\delta\overline{T_{out}})}{|\overline{T_{in}}-\overline{T_{out}}|}\right) \quad \text{[kW/K]} \qquad \text{Eq. (49)}$$

3. Building description

The previously proposed and explained method is now applied and developed in a real in-use building. The analysis has been done in a public building of the University of the Basque Country. The building is located on the Leioa University Campus, close to Bilbao, in the north of Spain.

For the analysis of the building HLC, it is indispensable to know about the climate of the area. Leioa has a humid oceanic climate with a predominance of the westerly winds, which softens the temperatures and favours a temperate time throughout the year. Due to the proximity to the sea, the climate is mild, however, it contrasts with the very marked temperature difference between seasons: 8ºC of average temperature in winter and 20ºC in summer. Hence, while the summers are comfortable, the winters are long, cold, wet and windy and it is partly cloudy all year round.

As detailed in section 2, the proposed HLC estimation method requires data periods with very specific weather conditions. As an example of a suitable period fulfilling those requirements, the data from period 2 of winter 2014-2015 is analysed here (period from 15/1/20 to 15/1/23). This period's data is plotted in [26], where the internal and external temperature are shown in Fig. 3 and the horizontal and vertical global solar radiation are shown in Fig. 5. Moreover, Table A.1 and Table A.3 from Appendix

A show the average values of each of the main variables of all the selected periods. These values can be used directly to estimate the HLC values using the Eq. (49) form for HLC estimation (in this equation the variables are introduced as the average of the selected period). Thus, if the T_{out} column of Table A.1 and the S_aV_{sol} column of Table A.3 are observed, for the period 2 example, a low external temperature (6.23 ºC) and low solar gains (8.76 kW) average values can be observed. These weather conditions permit the high indoor to outdoor temperature difference and the low solar gains conditions required by the method to be fulfilled.

3.1. Description of the building before the retrofitting

The building presents a complex geometry, with an irregular façade and projecting parts on different levels. The building is formed by three different blocks, but only the west block has been considered in the energy characterization. The whole building has the same heating system. Each block has four storeys and has a narrow layout with a structure of concrete pillars and grid concrete slabs. The distribution of the floor is explained in [26], where F1 and F3 are open areas, while different smaller rooms and offices make up F0 and F2. The building has a centralized heating system, but before retrofitting, it did not have ventilation or air conditioning facilities.

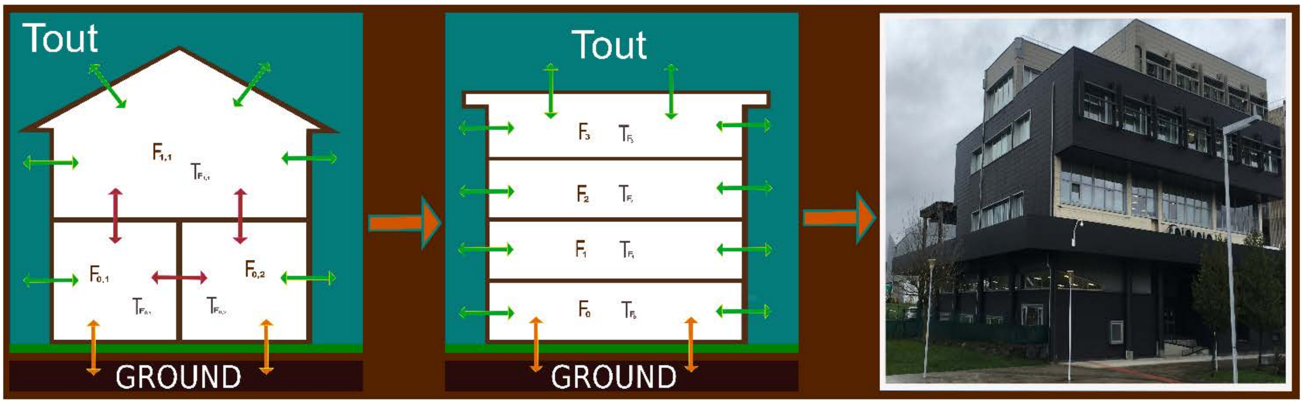

Figure 3. Left: generic building schematic used for method demonstration. Centre: from the generic building schematic to the schematic of the studied building. Right: photo of the studied building after retrofitting.

The building was constructed in the 1970s without insulation. During its life, it has been modified several times. Regarding the opaque walls, the majority of the façade was built with precast concrete panels without an air gap. There were three kinds of window in the building; wooden frame and single glazed windows, aluminium frame (without thermal break) and double glazed windows and, finally, aluminium frame (with thermal break) and double glazed windows. Some of the windows had concrete-sunshades to reduce solar gains during summer. Moreover, the roof was partially insulated.

Section 2.2 demonstrates that the HLC estimation of the building can be done as if each of the analysed zones are exchanging heat and mass only with the outdoors. The heat and mass exchange between the internal walls and ceilings are cancelled out when performing the Eq. (41) sum. Then, the considered energy exchange schema of the presented building is shown in Figure 3 (centre). Therefore, four HLC values will be calculated, one for each floor of the building.

3.2. Description of the building after the retrofitting

The retrofitting works were designed during the year 2015, and the works were started in summer 2016. A monitoring study was carried out before these works in order to make a diagnosis of the building and this was taken into account to define the optimal retrofitting actions.

The main objective of the retrofitting was to decrease the building's energy consumption. Therefore, the first step carried out to achieve this aim was to reduce the energy demand through the reduction of the building's envelope energy losses. Furthermore, improvements in the energy systems of the building were also considered.

Thus, several actions were carried out to reduce the energy consumption and CO_2 emissions of the building. The first action developed was the retrofitting of the façade, which has been insulated by adding vacuum insulated panels (VIPs) within a ventilated façade. Moreover, a new lighting system has been installed, where natural and LED lights were combined as well as a control system for it. Some windows have also been replaced by a new type of reversible window and others by market available high performance windows with different solar behaviour, depending on the orientation.

In addition, a ventilation system with recovery has been installed for each floor, with its control system and thermostatic control valves on the hot water radiators in order to improve the control capacities.

3.3. Description of the monitoring system of the building

Different types of sensors have been located all around the building, depending on the distribution of each plant (see Table 1). Three different types of monitoring systems have been installed: sensors measuring the external conditions, sensors measuring the indoor conditions and, finally, sensors measuring the building's energy consumption. The external measurements include the brightness level on the roof, temperature (two sensors), relative humidity (two sensors), wind speed, wind direction and horizontal global solar radiation. One outdoor CO_2 concentration sensor has been installed after the retrofitting. The interior sensors are also able to measure the brightness level, temperature, relative humidity and air quality (CO_2 concentration). Finally, the energy consumption of the heating systems is obtained, since the heating water flow rate, the flow temperature and the return temperature are measured for each floor. On the other hand, it is also possible to obtain the electricity consumption by measuring the active power consumption in each floors' electrical board.

Although most of the data has been obtained by the sensors directly, some parameters have been estimated for the HLC estimation. The estimation of the total solar aperture of the building ($S_a = 230.15\ m^2$) is justified in [26]. The distribution of the solar aperture through the different floors has been done proportionally to the total window area of each floor: the ground floor has 16%, the first floor has 36%, the second floor 23% and the third floor 25% of the whole solar aperture. As shown in Table 1, the measured solar radiation is the Global Horizontal Solar Radiation (H_{sol}).

Sensors	Accuracy	Measure Type	
7 Calorimeter: Kamstrup Multical 602 for heating; F0 1 calorimeter; F1, F2 and F3 2 calorimeters per floor	E_T ± (0.4 + 4/ΔT)% for the set sensors	Heating system	**Energy consumption**
4 Electricity Power Meter: 1 ABB EM/S 3.16.1 meter, 3 ABB A43 meters (1 per floor)	±2% for all	Lighting system	
13 Illuminance sensors: Siemens 5WG1 255-4AB12	-	Illuminance (lux)	**Indoor Conditions**
13 Air quality, Temperature and Humidity Sensors: ARCUS SK04-S8-CO_2-TF	±1% Measurement Error	Air Quality (ppm CO_2)	
	±0.5 °C	Temperature (°C)	
	±3% RH	Relative Humidity (%)	
1 Weather Station on roof: ELSNER 3595 Sun tracer KNX basic	±35% at 0…150,000 lux	Illuminance (lux)	**Weather**
	±0.5 °C	Temperature (°C)	
	±25% at 0…15 m/s	Wind Speed (m/s)	
	-	Rain (yes/no)	
1 Outdoors Temperature and Humidity Sensor on roof ARCUS SK01-TFK-AFF	±0.5 °C	Temperature (°C)	
	±3% RH	Relative Humidity (%)	
1 Pyranometer on roof: ARCUS SK08-GLBS	±5%	Global Horizontal Solar Radiation (W/m^2)	

Table 1. Summary of the analysed building's sensors.

During this study, the internal gains have been estimated as in [26] in order to estimate the occupancy heat created by people's metabolic generation and the heat generated by the computers. This procedure is applied floor by floor, considering the people and computers working on each of them. The considered occupancy scheduled for each floor has been estimated by means of interviews and by analysing the measured lighting consumption data sets.

4. Results and discussion

The presented in-use office building was monitored from November 2014 to March 2018; every November-April period were studied. Within each of these four winter periods, useful data periods (at least 72h sub-periods) were identified in which the Section 2 requirements are completely fulfilled. Once all these sub-periods had been detected, the proposed accumulated average method was applied floor by floor, and for the whole building, to all of them. Then, those values were compared to check the variation of the estimated HLCs and demonstrate the reliability of the method. If the method is valid, the HLC of the whole building should not vary much over time. Note that the estimated HLCs are independent of each other, since different periods of data are used within the same winter and, in the pre-retrofitting case, even the HLCs estimated in different winters are comparable.

In this section, the change of the Heat Loss Coefficient value for the pre- and post-retrofitting is also studied. Therefore, two different sections are presented. The first section analyses the HLC of the public building before retrofitting. Thus, it can be checked whether the HLC values have been changing over time or whether they are similar, since the building did not undergo any known improvement or deterioration during this period. On the other hand, the second section studies how the HLC value has changed after the retrofitting of the building. The value is expected to decrease due to the improved insulation and new ventilation systems with heat recovery being installed in the building.

4.1. Pre-Retrofitting HLC Results

The results obtained for the valid sub-periods of the three winters between November 2014 and April 2017 are analysed in this section. In order to estimate the Heat Loss Coefficients of the building envelope before the retrofitting, Eq. (25) has been used to estimate the HLC, while Eq. (26) has been used to estimate the HLC_{simple}. In total, eight valid periods have been found for the three winters, as shown in Table 2 and Table 3, where estimated HLC_{simple} and HLC for each valid period are presented. Appendix A shows the average value of each of the terms of Eq. (25) and Eq. (26) applied to each period, while Appendix B shows the ±10% stabilization bands of some period's accumulated average with respect to the final HLC estimate. Moreover, the calculations have been done floor by floor and for the whole building. Thus, it is possible to compare the difference when estimating the HLC directly for the whole building's averaged data ($HLC_{building}$) or as a sum of the floor by floor HLCs (HLC_{sum}).

$HLC_{Simple} = \frac{\sum_{k=1}^{N}(Q_k + K_k)}{\sum_{k=1}^{N}(T_{in,k} - T_{out,k})}$ [kW/K] Eq. (26)				FLOOR 0 Eq. (39)	FLOOR 1 Eq. (39)	FLOOR 2 Eq. (39)	FLOOR 3 Eq. (39)	HLC_{Sum} Eq. (27)	$HLC_{Building}$ Eq. (46)
Winter	From	To	Total Hours	$HLC_{F0} \pm e_{HLC_{F0}}$	$HLC_{F1} \pm e_{HLC_{F1}}$	$HLC_{F2} \pm e_{HLC_{F2}}$	$HLC_{F3} \pm e_{HLC_{F3}}$	$HLC_{sum} \pm e_{HLC_{sum}}$	$HLC_{building} \pm e_{HLC_{building}}$
2014-2015	14/12/2/ 16:00	14/12/5/ 20:00	77	0.82 ± 0.08	1.36 ± 0.12	0.97 ± 0.08	1.16 ± 0.10	4.32 ± 0.38	4.34 ± 0.38
	15/1/20/ 10:00	15/1/23/ 8:00	72	0.95 ± 0.08	1.46 ± 0.12	1.06 ± 0.08	1.27 ± 0.10	4.74 ± 0.39	4.76 ± 0.39
	15/1/26/ 19:00	15/1/30/ 20:00	99	1.06 ± 0.12	1.55 ± 0.17	1.05 ± 0.10	1.30 ± 0.13	4.96 ± 0.52	4.97 ± 0.52
	15/2/3/ 6:00	15/2/7/ 1:00	93	0.97 ± 0.08	1.40 ± 0.11	0.98 ± 0.07	1.19 ± 0.09	4.53 ± 0.35	4.54 ± 0.34
2015-2016	15/11/24/ 19:00	15/11/27/ 22:00	76	0.97 ± 0.13	1.60 ± 0.15	1.11 ± 0.11	1.34 ± 0.13	5.02 ± 0.51	5.10 ± 0.52
	16/1/6/ 20:00	16/1/9/ 8:00	61	0.98 ± 0.17	1.44 ± 0.23	0.99 ± 0.16	1.30 ± 0.21	4.72 ± 0.77	4.75 ± 0.77
2016-2017	16/12/19/ 12:00	16/12/22/ 6:00	67		1.34 ± 0.13	0.98 ± 0.09	1.20 ± 0.11	3.51 ± 0.34	3.51 ± 0.34
	17/1/9/ 18:00	17/1/12/ 7:00	62		1.07 ± 0.13	0.91 ± 0.10	1.08 ± 0.13	3.05 ± 0.36	3.05 ± 0.36

Table 2. HLC_{simple} results before retrofitting.

$HLC = \frac{\sum_{k=1}^{N}(Q_k + K_k + (S_a V_{sol})_k)}{\sum_{k=1}^{N}(T_{in,k} - T_{out,k})}$ [kW/K] Eq. (25)				FLOOR 0 Eq. (40)	FLOOR 1 Eq. (40)	FLOOR 2 Eq. (40)	FLOOR 3 Eq. (40)	HLC_{sum} Eq. (27)	$HLC_{building}$ Eq. (46)
Winter	From	To	Total Hours	$HLC_{F0} \pm e_{HLC_{F0}}$	$HLC_{F1} \pm e_{HLC_{F1}}$	$HLC_{F2} \pm e_{HLC_{F2}}$	$HLC_{F3} \pm e_{HLC_{F3}}$	$HLC_{sum} \pm e_{HLC_{sum}}$	$HLC_{building} \pm e_{HLC_{building}}$
2014-2015	14/12/2/ 16:00	14/12/5/ 20:00	77	0.91 ± 0.10	1.53 ± 0.16	1.08 ± 0.11	1.28 ± 0.12	4.80 ± 0.49	4.83 ± 0.49
	15/1/20/ 10:00	15/1/23/ 8:00	72	1.04 ± 0.09	1.64 ± 0.15	1.18 ± 0.09	1.39 ± 0.12	5.25 ± 0.45	5.28 ± 0.45
	15/1/26/ 19:00	15/1/30/ 20:00	99	1.14 ± 0.14	1.70 ± 0.20	1.14 ± 0.12	1.40 ± 0.16	5.38 ± 0.61	5.40 ± 0.60
	15/2/3/ 6:00	15/2/7/ 1:00	93	1.03 ± 0.08	1.54 ± 0.12	1.07 ± 0.08	1.28 ± 0.10	4.93 ± 0.38	4.94 ± 0.38
2015-2016	15/11/24/ 19:00	15/11/27/ 22:00	76	1.04 ± 0.14	1.73 ± 0.17	1.19 ± 0.12	1.42 ± 0.14	5.39 ± 0.66	5.47 ± 0.57
	16/1/6/ 20:00	16/1/9/ 8:00	61	1.06 ± 0.19	1.60 ± 0.27	1.09 ± 0.18	1.41 ± 0.24	5.17 ± 0.89	5.20 ± 0.90
2016-2017	16/12/19/ 12:00	16/12/22/ 6:00	67		1.49 ± 0.16	1.08 ± 0.11	1.31 ± 0.14	3.87 ± 0.42	3.87 ± 0.43
	17/1/9/ 18:00	17/1/12/ 7:00	62		1.13 ± 0.14	0.95 ± 0.11	1.12 ± 0.13	3.20 ± 0.36	3.19 ± 0.39

Table 3. HLC results before retrofitting.

As expected, from the above tables, it can be concluded that the HLC value has barely changed during the independent periods considered in three consecutive winters, since all the estimated HLC_{simple} values are close to the average value 4.75 ± 0.49 kW/K with a standard deviation of 0.28 kW/K. For the HLC, the average value is 5.18 ± 0.56 kW/K with a standard deviation of 0.25 kW/K.

There is a lack of data on the ground floor during the winter of 2016-2017, which made it impossible to estimate its HLC during the two valid periods considered during this winter. However, the estimation has been carried out for the rest of the floors. Since the indoor average temperature of all the periods is similar on all the floors (see Appendix A), it is possible to estimate an HLC value for the ground floor for the winter of 2016-2017. The average value of 0.96 ± 0.11 kW/K for the HLC_{simple} and 1.04 ± 0.12 kW/K for the HLC of the ground floor is obtained by averaging the 6 available periods of the winters 2014-2016. Thus, an average value of all the HLC_{sum} of 4.25 ± 0.46 kW/K for the HLC_{simple} and 4.56 ± 0.53 kW/K for the HLC for the winter of 2016-2017 would be obtained. These are within the error bands of the total HLC average values obtained for the winters 2014-2016. However, the latter estimated values cannot be considered as completely reliable, since during the summer of 2016 the ground floor's false ceiling was insulated.

Moreover, the HLC values are higher than the HLC_{simple} values estimated without considering the solar gains. On the other hand, the difference is below 10%, since low solar radiation periods have been considered to avoid a considerable error in the results due to roughly estimated solar gains, as detailed in Section 2.1.

It should also be mentioned that the difference between the summed HLC (HLC_{sum} in Table 2 and Table 3) and the total HLC values ($HLC_{building}$ in Table 2 and Table 3) have similar values. Since the T_{in} is uniform on the different floors for all periods, the deviation between HLC_{sum} and $HLC_{building}$ is negligible. Nevertheless, since the measurements floor by floor can be obtained, the results obtained from these will always be more accurate than the result obtained for the whole building. Therefore, the HLC_{sum} value should be taken as reference.

To sum up, the HLC value of 5.18 ± 0.56 kW/K is considered the best estimate for the HLC of the building before the retrofitting.

4.2. *Post-Retrofitting HLC Results*

The same procedure is followed to estimate the HLC_{simple} and the HLC for the winter of 2017-2018. These calculations have been carried out after the energy retrofitting of the public building. Since the building use has been kept identical in the post-retrofitting case, the same occupancy estimation as for Section 4.1 has been assumed for occupancy heat gains. Thus, since the building has been insulated properly, the HLC should have decreased considerably.

$HLC_{simple} = \frac{\sum_{k=1}^{N}(Q_k + K_k)}{\sum_{k=1}^{N}(T_{in,k} - T_{out,k})}$ [kW/K] Eq. (26)				FLOOR 0 Eq. (39)	FLOOR 1 Eq. (39)	FLOOR 2 Eq. (39)	FLOOR 3 Eq. (39)	HLC_{Sum} Eq. (27)	$HLC_{Building}$ Eq. (46)
Winter	From	To	Total Hours	$HLC_{F0} \pm e_{HLC_{F0}}$	$HLC_{F1} \pm e_{HLC_{F1}}$	$HLC_{F2} \pm e_{HLC_{F2}}$	$HLC_{F3} \pm e_{HLC_{F3}}$	$HLC_{sum} \pm e_{HLC_{sum}}$	$HLC_{building} \pm e_{HLC_{building}}$
2017-2018	17/11/6/ 18:00	17/11/10/ 9:00	88	0.60 ± 0.07	0.94 ± 0.09	0.64 ± 0.06	0.66 ± 0.08	2.83 ± 0.31	2.85 ± 0.30
	17/11/26/ 21:00	17/12/2/ 12:00	136	0.60 ± 0.05	1.06 ± 0.09	0.63 ± 0.06	0.70 ± 0.07	2.99 ± 0.26	3.00 ± 0.27
	17/12/20/ 9:00	17/12/23/ 9:00	73	0.62 ± 0.06	1.06 ± 0.10	0.63 ± 0.06	0.78 ± 0.08	3.10 ± 0.29	3.10 ± 0.29
	18/1/17/ 4:00	18/1/20/ 6:00	75	0.63 ± 0.06	1.06 ± 0.10	0.69 ± 0.06	0.87 ± 0.08	3.25 ± 0.30	3.27 ± 0.30
	18/2/6/ 17:00	18/2/10/ 7:00	87	0.57 ± 0.04	0.94 ± 0.08	0.64 ± 0.05	0.71 ± 0.06	2.86 ± 0.23	2.85 ± 0.23

Table 4. HLC_{simple} results after retrofitting.

$HLC = \frac{\sum_{k=1}^{N}(Q_k + K_k + (S_a V_{sol})_k)}{\sum_{k=1}^{N}(T_{in,k} - T_{out,k})}$ [kW/K] Eq. (25)				FLOOR 0 Eq. (40)	FLOOR 1 Eq. (40)	FLOOR 2 Eq. (40)	FLOOR 3 Eq. (40)	HLC_{sum} Eq. (27)	$HLC_{building}$ Eq. (46)
Winter	From	To	Total Hours	$HLC_{F0} \pm e_{HLC_{F0}}$	$HLC_{F1} \pm e_{HLC_{F1}}$	$HLC_{F2} \pm e_{HLC_{F2}}$	$HLC_{F3} \pm e_{HLC_{F3}}$	$HLC_{sum} \pm e_{HLC_{sum}}$	$HLC_{building} \pm e_{HLC_{building}}$
2017-2018	17/11/6/ 18:00	17/11/10/ 9:00	88	0.77 ± 0.09	1.29 ± 0.17	0.88 ± 0.11	0.96 ± 0.15	3.90 ± 0.52	3.92 ± 0.52
	17/11/26/ 21:00	17/12/2/ 12:00	136	0.71 ± 0.06	1.28 ± 0.10	0.77 ± 0.06	0.86 ± 0.08	3.61 ± 0.30	3.62 ± 0.32
	17/12/20/ 9:00	17/12/23/ 9:00	73	0.75 ± 0.08	1.32 ± 0.15	0.80 ± 0.09	0.97 ± 0.12	3.84 ± 0.44	3.85 ± 0.44
	18/1/17/ 4:00	18/1/20/ 6:00	75	0.76 ± 0.08	1.33 ± 0.15	0.86 ± 0.10	1.07 ± 0.13	4.03 ± 0.46	4.04 ± 0.46
	18/2/6/ 17:00	18/2/10/ 7:00	87	0.65 ± 0.05	1.11 ± 0.10	0.74 ± 0.07	0.83 ± 0.08	3.32 ± 0.30	3.32 ± 0.30

Table 5. HLC results after retrofitting.

In Section 4.1, the obtained average values were 4.75 ± 0.49 kW/K for the HLC_{simple} and 5.18 ± 0.56 kW/K for the HLC. On the other hand, the obtained average values during the winter 2017-2018 periods are 3.01 ± 0.27 kW/K for the HLC_{simple} with a standard deviation of 0.18 kW/K and 3.74 ± 0.41 kW/K for the HLC with a standard deviation of 0.28 kW/K. Thus, the reduction has been considerable for the HLC value, considering that the façade has been insulated and some of the windows changed, while the ventilation system with heat recovery has increased the ventilation rates. The combined effect is a reduction of 28% in the HLC.

To sum up, the HLC value of 3.74 ± 0.41 kW/K is considered the best estimate for the HLC of the building after the retrofitting.

4.3. Discussion

The whole building's HLC results are plotted in the following figures:

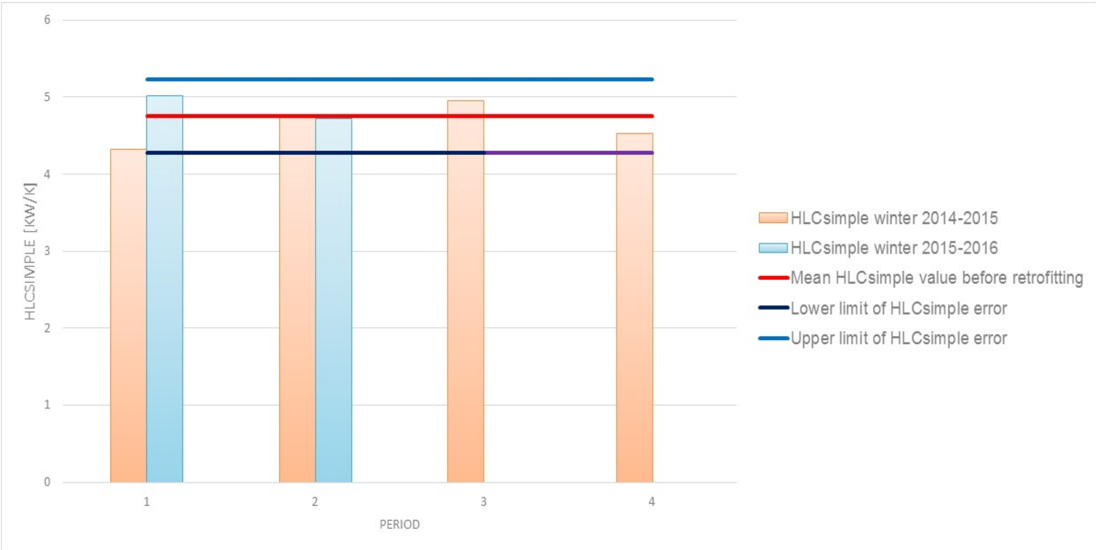

Figure 4. HLC_{simple} values before retrofitting (winter 2014-2015 and winter 2015-2016).

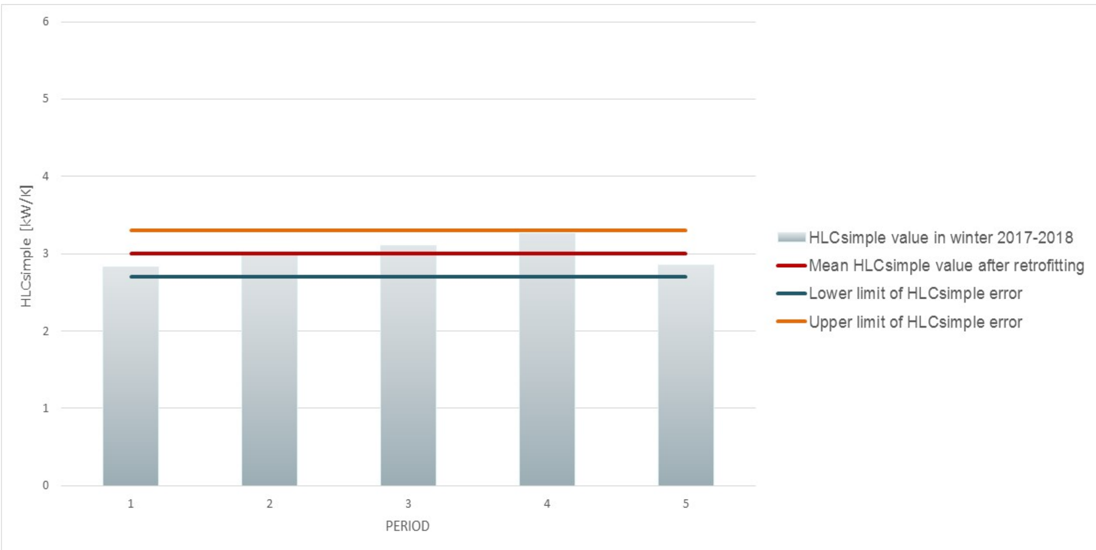

Figure 5. HLC_{simple} values after retrofitting (winter 2017-2018).

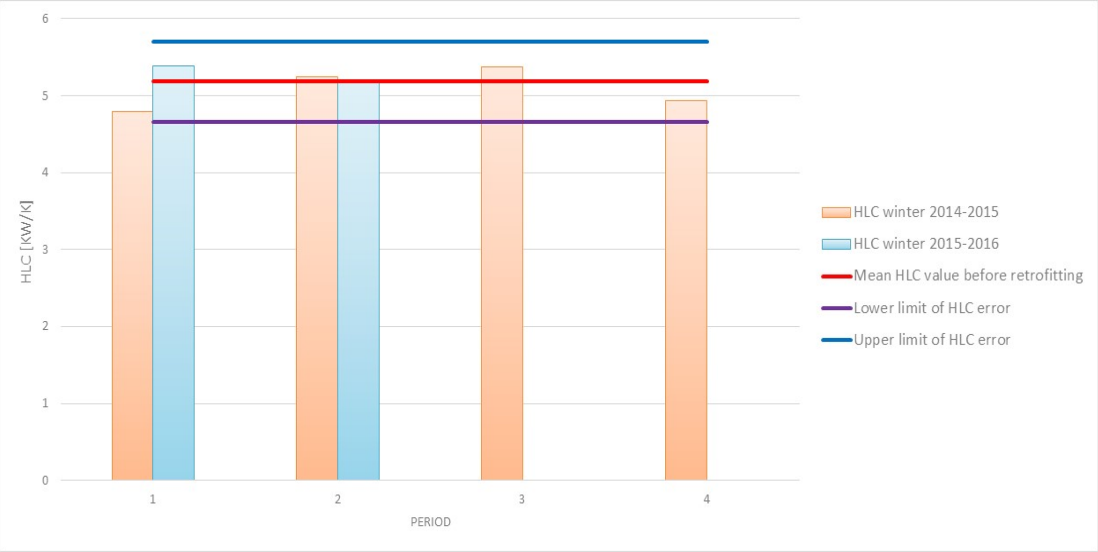

Figure 6. HLC values before retrofitting (winter 2014-2015 and winter 2015-2016).

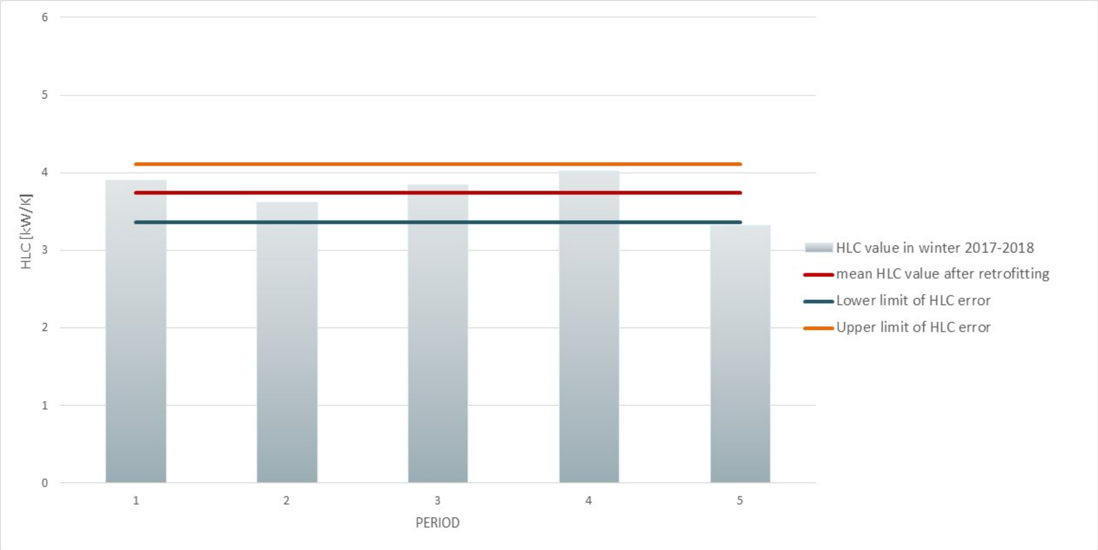

Figure 7. HLC values after retrofitting (winter 2017-2018).

As commented in the previous section, several conclusions can be drawn from the graphics. First of all, it is important to check that all the periods, before and after retrofitting, show similar results. From these figures, it can be concluded that almost all the individual HLC_{simple} or HLC estimates are within the corresponding average value, plus or minus the error band.

Only the fifth period of winter 2017-2018 (Figure 7) was not able to reach the error band limits of the estimated HLC average value. However, this estimate is not differing considerably from the rest of the values since the lower error limit is 3.36 kW/K while the fifth period HLC estimate is 3.32 kW/K.

Moreover, the values obtained by estimating the HLC with and without considering the solar radiation do not differ by much. While the average value for the pre-retrofit HLC_{simple} was 4.75 kW/K, the HLC value considering solar radiation increases to 5.18 kW/K. These two results only differ by 8.3% thanks to the proposed data period selection procedure described in Section 2.1. It is very difficult to estimate the real solar gains entering the building due to the unmeasurable effects of such elements as blinds or curtains located in windows, which are the main obstacle when making an estimation of solar gains. Therefore, by selecting cloudy and cold days, the unreliable in-use solar gain effect on the HLC estimate can be limited to below 10%, which would be the limiting case of not considering the solar gains effect, as in Eq. (26). By using Eq. (25), although roughly estimating the solar gains, the uncertainty effect on the HLC will be below 10%. However, solar gains effects in the post-retrofitted HLC estimation are higher, while the HLC_{simple} value was 3.01 kW/K, the HLC increased until 3.74 kW/K. These two values differ by 20%. As expected, for correctly insulated buildings, the solar gains effect on the HLC is greater. In insulated buildings, the heating demand decreases and thus, the same amount of solar gains will produce a bigger difference between the HLC_{simple} and the HLC.

Finally, as commented previously, when estimating the HLC before and after the retrofitting, a considerable drop can be observed. If all valid period average HLC_{sum} values are compared, it can be seen that the HLC_{simple}, when not considering solar radiation, has decreased by 1.74 kW/K (36%), while the HLC, considering solar gains, has decreased by 1.44 kW/K (28%).

As detailed in Section 2.1, the HLC = UA + C_v and thus it considers: transmission (UA) plus infiltration (C_v as in Eq. (5)) for the periods considered in the pre-retrofitting case; while for the post-retrofitting case, the HLC considers the transmission effects (UA) plus infiltration plus ventilation with heat recovery effects (C_v as in Eq. (13)) for the post-retrofitted case. The UA value can be considered constant for all pre-retrofitted periods and it can also be considered constant for all the post-retrofitted periods.

During the pre-retrofitted periods, the C_v value only considers the infiltration effects and these effects might vary mainly due to wind speed and indoor to outdoor temperature difference variations. Note that using the proposed method, the estimated HLC value considers the average C_v value of each of the studied periods; so C_v values between periods might be different. Thus, part of the noise in the HLC estimates of the pre-retrofitted case might be due to variations in the C_v part of each independent period. It is very important to develop procedures to decouple the HLC into UA and C_v values. For the estimation of the infiltration C_v detailed in Eq. (5), the use of metabolic CO_2 decay analysis might be a cost-effective option.

For the post-retrofitted case, the new UA value can be assumed to be constant for all the studied periods. However, the ventilation plus infiltration C_v value will be dependent on both: the regulation of the ventilation system and the behaviour of the infiltrations, which are mainly dependent on the wind velocity and indoor to outdoor temperature variations. Again, the method provides an HLC value that embeds the period averaged C_v value for the analysed period. Here, the decoupling process would be harder, since we have both infiltrations plus ventilation with heat recovery. For such cases, the heat recovery system should also be monitored to measure the inlet and outlet flow rates, together with the supply temperature and the temperature of the air leaving the heated space. With these values, it would be possible to calculate the part of the C_v due to the ventilation system for the analysed period. For the infiltration part, the metabolic CO_2 decay method could be applied to obtain the total ventilation rates. Then, the ventilation system's ventilation rate could be subtracted from the total ventilation rate to obtain the infiltration part of the total ventilation rate. Thus, the C_v part due to the infiltrations could also be estimated and the total C_v value, presented in detail in Eq. (13), could be estimated.

However, for both the pre-retrofit (5.18 kW/K ± 10.8%) and post-retrofit (3.74 kW/K ± 10.9%) cases, all independent periods have estimated the HLC_{sum} values within the corresponding error band, as compared to the average of all estimated HLC_{sum}. This leads us to conclude that the infiltration behaviour has been similar for all the periods analysed during the pre-retrofit case and the infiltration plus ventilation behaviour have also been similar for all periods analysed in the post-retrofitting case. The latter can be partially corroborated, since the ventilation part has been operating on the same schedule, with constant ventilation rates for all the working days of the winter of 2017-2018. The method leads us to use periods where heating gains are high and thus, indirectly, all selected periods consider only working days where the heating system is ON and the ventilation system patterns are similar.

Finally, in order to verify the results, it was in mind the possibility to compare the average method results with the results of an established method. Therefore, it was considered that the Co-heating method [20] could play an important role in this comparison. However, due to the size and the geometry of the building, it has been unfeasible to apply the Co-heating method in the analysed building. Furthermore, since winter period is not a holyday period, it was inviable to empty the whole building during one month in any of the studied winters for applying the Co-heating method. However, this average method has been tested by the paper research team within the IEA-EBC ANNEX71 'Building energy performance assessment based on in situ measurements' of the EBC (Energy in Buildings and Communities Program) of the IEA (International Energy Agency) to estimate the HLC of the Loughborough single zone case study house. The HLC estimate of the UPV/EHU team for the Loughborough case under in-use conditions have been 367 ± 28W/K while the Co-heating HLC value [32] was 382 W/K.

5. Conclusions

This paper proves the validity of the proposed average method by developing it from the First Law of Thermodynamics in order to provide the method with the suitable assumptions to work with in-use buildings. The proposed method has then been applied to an in-use building monitored over four years to estimate its Heat Loss Coefficient in all the independent periods suitable for the method's application.

Following the method's indications, a successful estimation of the Heat Loss Coefficient has been achieved for both; the pre-retrofitted building and the post-retrofitted building. The periods between November 2014 and April 2017 were first studied. During this period, the building had not yet been retrofitted, so the obtained averaged results were 4.75 ± 0.49 kW/K for the HLC_{simple} and 5.18 ± 0.56 kW/K for the HLC. However, during the summer of 2017, the building was retrofitted and the envelope of the building insulated. Furthermore, a ventilation system with heat recovery was also installed. Therefore, a considerable drop can be observed in the HLC, since the values attained between November 2017 and March 2018 were 3.01 ± 0.27 kW/K for the HLC_{simple} and 3.74 ± 0.41 kW/K for the HLC. The values considered most reliable are those obtained from the floor by floor sum (HLC_{sum}), since they consider more accurate data, rather than a single estimated HLC value for the whole building ($HLC_{building}$). Hence, the HLC has decreased 28% after the retrofitting from the pre-retrofit case of 5.18 kW/K to the post-retrofitted case of 3.74 kW/K.

Moreover, it can be also concluded that all the individual estimates of HLC_{simple} and HLC were able to obtain similar results for winters before and after the retrofitting. The method itself is able to provide accurate results without the requirement of a physical model of the building.

After the retrofitting, some extra sensors were installed in the building. One of these sensors was the total electricity consumption measurer per floor. This means that it is currently possible to measure the electricity demand of each occupant (computers, own electrical devices…). However, it is still necessary to estimate the person's metabolic generation, since it is hard to measure this on site. Therefore, the proposal for further research is to estimate the Heat Loss Coefficient using the measured total electricity consumption and to compare the final results with those obtained in this paper. The difference is expected to be small, since the weight of the occupancy heat gains is small during the cold and cloudy periods considered in this work for HLC estimations, where heating demands are highest. Moreover, the development of HLC decoupling methods will have to be developed so as to be able to obtain the UA value embedded in the estimated HLC values. Then, the UA values could be compared with the design ones. This could lead to more realistic energy certificates in buildings in so far as the building envelope is concerned.

6. Acknowledgments

This work was supported by the Spanish Economy and Competitiveness Ministry and the European Regional Development Fund through the IMMOEN project 'Implementation of automated calibration and multiobjective optimization techniques applied to Building Energy Model simulations by means of monitored buildings', project reference: ENE2015-65999-C2-2-R and ENE2015-65999-C2-1-R (MINECO/FEDER); by the European Commission through the A2PBEER project 'Affordable and Adaptable Public Buildings through Energy Efficient Retrofitting', Grant agreement no: 609060; by the University of the Basque Country (UPV/EHU) by providing funding and the studied in-use office building. The corresponding author also acknowledges the support provided by the Education Department of the Basque Government through a scholarship granted to her to complete her PhD degree.

References

[1] European Commission, Energy Performance of Buildings Directive (EPBD) Compliance Study. 2018, https://ec.europa.eu/energy/en/studies/energy-performance-buildings-directive-epbd-%E2%80%93-study-compliance (2015).

[2] H2020 Energy Efficient Buildings (EeB), http://ec.europa.eu/research/industrial_technologies/energy-efficient-buildings_en.html (2018).

[3] EU Buildings Factsheets, https://ec.europa.eu/energy/en/eu-buildings-factsheets (2018).

[4] E. Burman, D. Mumovic, J. Kimpian, Towards measurement and verification of energy performance under the framework of the European directive for energy performance of buildings, Energy. 77 (2014), 153-163 //doi.org/10.1016/j.energy.2014.05.102.

[5] "Intelligent Energy-Europe", Implementing of the Energy Performance of Buildings directive (EPBD), Co-funded under the Intelligent Energy-Europe Programme of the European Union (2015).

[6] A.J. Summerfield, T. Oreszczyn, I.G. Hamilton, D. Shipworth, G.M. Huebner, R.J. Lowe, P. Ruyssevelt, Empirical variation in 24-h profiles of delivered power for a sample of UK dwellings: Implications for evaluating energy savings, Energy and Buildings. 88 (2015), 193-202 //doi.org/10.1016/j.enbuild.2014.11.075.

[7] M.J. Jiménez, M.R. Heras, Application of multi-output ARX models for estimation of the U and g values of building components in outdoor testing, Solar Energy. 79 (2005); 302-310//doi.org/10.1016/j.solener.2004.10.008.

[8] M.J. Jiménez, B. Porcar, M.R. Heras, Estimation of building component UA and gA from outdoor tests in warm and moderate weather conditions, Solar Energy. 82 (2008), 573-587 //doi.org/10.1016/j.solener.2008.02.013.

[9] K.K. Andersen, H. Madsen, L.H. Hansen, Modelling the heat dynamics of a building using stochastic differential equations, Energy and Buildings. 31 (2000), 13-24 //doi.org/10.1016/S0378-7788(98)00069-3.

[10] P. Bacher, H. Madsen, Identifying suitable models for the heat dynamics of buildings, Energy and Buildings. 43 (2011); 1511-1522//doi.org/10.1016/j.enbuild.2011.02.005.

[11] N.R. Kristensen, H. Madsen, S.B. Jørgensen, Parameter estimation in stochastic grey-box models, Automatica. 40 (2004), 225-237 //doi.org/10.1016/j.automatica.2003.10.001.

[12] S. Roels, P. Bacher, G. Bauwens, H. Madsen, M.J. Jiménez, Characterising the Actual Thermal Performance of Buildings: Current Results of Common Exercises Performed in the Framework of the IEA EBC Annex 58-Project, Energy Procedia. 78 (2015); 3282-3287//doi.org/10.1016/j.egypro.2015.11.726.

[13] X. Lü, T. Lu, C.J. Kibert, M. Viljanen, Modeling and forecasting energy consumption for heterogeneous buildings using a physical–statistical approach, Appl. Energy. 144 (2015); 261-275.

[14] P. De Wilde, The gap between predicted and measured energy performance of buildings: A framework for investigation, Automation in Construction. 41 (2014), 40-49 //doi.org/10.1016/j.autcon.2014.02.009.

[15] C. Aghemo, J. Virgone, G.V. Fracastoro, A. Pellegrino, L. Blaso, J. Savoyat, K. Johannes, Management and monitoring of public buildings through ICT based systems: Control rules for energy saving with lighting and HVAC services, Frontiers of Architectural Research. 2 (2013), 147-161 //doi.org/10.1016/j.foar.2012.11.001.

[16] F. Stevenson, H.B. Rijal, Developing occupancy feedback from a prototype to improve housing production, Build. Res. Inf. 38 (2010); 549-56310.1080/09613218.2010.496182.

[17] P. Eguía Oller, J.M. Alonso Rodríguez, Á Saavedra González, E. Arce Fariña, E. Granada Álvarez, Improving transient thermal simulations of single dwellings using interpolated weather data, Energy and Buildings. 135 (2017), 212-224 //doi.org/10.1016/j.enbuild.2016.11.030.

[18] D. Johnston, D. Farmer, M. Brooke-Peat, D. Miles-Shenton, Bridging the domestic building fabric performance gap, Build. Res. Inf. 44 (2016); 147-15910.1080/09613218.2014.979093.

[19] A.C. Menezes, A. Cripps, D. Bouchlaghem, R. Buswell, Predicted vs. actual energy performance of non-domestic buildings: Using post-occupancy evaluation data to reduce the performance gap, Appl. Energy. 97 (2012); 355-364.

[20] D. Butler, A. Dengel, Review of Co-heating Test Methodologies: Primary Research (2013).

[21] O. Mejri, E.P. Del Barrio, N. Ghrab-Morcos, Energy performance assessment of occupied buildings using model identification techniques, Energy Build. 43 (2011); 285-299.

[22] G. Bauwens, S. Roels, Co-heating test: A state-of-the-art, Energy Build. 82 (2014); 163-172.

[23] J. Chapman, R. Lowe, R. Everett, Pennyland project: executive summary.Final report (1985).

[24] M. Marzouk, N. Seleem, Assessment of existing buildings performance using system dynamics technique, Appl. Energy. 211 (2018); 1308-1323.

[25] X. Liang, T. Hong, G.Q. Shen, Improving the accuracy of energy baseline models for commercial buildings with occupancy data, Appl. Energy. 179 (2016); 247-260.

[26] A. Erkoreka, E. Garcia, K. Martin, J. Teres-Zubiaga, L. Del Portillo, In-use office building energy characterization through basic monitoring and modelling, Energy Build. 119 (2016); 256-266.

[27] M.J. Moran, H.N. Shapiro, D.D. Boettner, M.B. Bailey, Fundamentals of engineering thermodynamics, John Wiley & Sons, 2010.

[28] J.A. Duffie, W.A. Beckman, Solar engineering of thermal processes, John Wiley & Sons, 2013.

[29] J. Carmody, Residential windows: a guide to new technologies and energy performance (2007).

[30] ISO.Thermal insulation - Building elements - In-situ measurement of thermal resistance and thermal transmittance - Part 1: Heat flow meter method, ISO Standard 9869-1, AENOR, Genova, 2014.

[31] J.R. Taylor, Error analysis, Univ.Science Books, Sausalito, California (1997).

[32] A. Beizaee, D. Allinson, K.J. Lomas, E. Foda, D.L. Loveday, Measuring the potential of zonal space heating controls to reduce energy use in UK homes: The case of un-furbished 1930s dwellings, Energy Build. 92 (2015); 29-44.

I. Appendix A

The average values of all the required variables over the analysed periods have been calculated as in Eq. (47) and Eq. (48). The considered uncertainty of each variable is shown in Section 3.3 Moreover, the obtained results have been collected and reported in the following tables, floor by floor, for each period:

Before Retrofitting			Out	FLOOR 0		FLOOR 1		FLOOR 2		FLOOR 3		Building	
Winter	From	To	T_{out} [ºC]	T_{in} [ºC]	T_{in}-T_{out} [K]	T_{in} [ºC]	T_{in}-T_{out} [K]	T_{in} [ºC]	T_{in}-T_{out} [K]	T_{in} [ºC]	T_{in}-T_{out} [K]	T_{in} [ºC]	T_{in}-T_{out} [K]
2014-2015	14/12/2/ 16:00	14/12/5/ 20:00	8.74	22.30	13.55	24.39	15.65	24.69	15.94	24.79	16.05	24.05	15.33
	15/1/20/ 10:00	15/1/23/ 8:00	6.23	21.60	15.37	23.46	17.23	23.59	17.36	23.72	17.23	23.09	16.86
	15/1/26/ 19:00	15/1/30/ 20:00	9.93	21.57	11.64	23.08	13.15	23.50	13.57	23.70	13.77	22.96	13.03
	15/2/3/ 6:00	15/2/7/ 1:00	3.04	20.86	17.82	22.56	19.52	22.77	19.73	22.84	19.80	22.26	19.23
2015-2016	15/11/24/ 19:00	15/11/27/ 22:00	12.32	20.85	8.53	24.00	11.68	24.15	11.83	23.81	11.49	23.20	10.88
	16/1/6/ 20:00	16/1/9/ 8:00	13.68	20.45	6.77	21.69	8.01	21.62	7.94	21.39	8.01	21.29	7.61
2016-2017	16/12/19/ 12:00	16/12/22/ 6:00	9.00			23.23	14.11	23.39	14.28	23.32	14.20	23.31	14.20
	17/1/9/ 18:00	17/1/12/ 7:00	10.14			21.14	11.20	21.63	11.70	21.12	11.20	21.30	11.36

Table A.1. Average temperatures of each analysed period for winters 2014-2015, 2015-2016 and 2017-2018 before retrofitting.

Before Retrofitting			Out	FLOOR 0		FLOOR 1		FLOOR 2		FLOOR 3		Building	
Winter	From	To	T_{out} [ºC]	T_{in} [ºC]	T_{in}-T_{out} [K]	T_{in} [ºC]	T_{in}-T_{out} [K]	T_{in} [ºC]	T_{in}-T_{out} [K]	T_{in} [ºC]	T_{in}-T_{out} [K]	T_{in} [ºC]	T_{in}-T_{out} [K]
2017-2018	17/11/6/ 18:00	17/11/10/ 9:00	9.54	23.28	13.74	24.20	14.66	23.65	14.11	21.34	11.81	23.12	13.58
	17/11/26/ 21:00	17/12/2/ 12:00	6.22	23.21	16.99	24.11	17.90	24.50	18.28	23.54	17.33	23.84	17.62
	17/12/20/ 9:00	17/12/23/ 9:00	9.02	23.88	14.86	24.64	15.61	24.90	15.87	24.12	15.09	24.38	15.36
	18/1/17/ 4:00	18/1/20/ 6:00	9.20	23.64	14.44	24.53	15.33	24.70	15.50	23.86	14.66	24.18	14.98
	18/2/6/ 17:00	18/2/10/ 7:00	3.81	23.27	19.46	23.57	19.76	24.33	20.52	22.80	18.99	23.49	19.68

Table A.2. Average temperatures of each analysed period for winter 2017-2018 after retrofitting.

Winter	Before Retrofitting		Q [kW]	K [kW]	Q+K [kW]	SaVsol ~ SaHsol [kW]	Tin-Tout [K]	HLC [kW/K]
2014 - 2015	Period 1 14/12/02 16:00 - 14/12/05 20:00	Floor 0	8.08	3.02	11.10	1.18	13.55	0.91
		Floor 1	13.43	7.92	21.35	2.67	15.65	1.53
		Floor 2	11.23	4.27	15.50	1.70	15.94	1.08
		Floor 3	13.34	5.31	18.65	1.85	16.05	1.28
		HLC_{sum}	46.07	20.52	66.59	7.41	15.30	4.80
		$HLC_{building}$	46.07	20.52	66.59	7.41	15.33	4.83
	Period 2 15/01/20 10:00 - 15/01/23 8:00	Floor 0	11.55	3.05	14.61	1.40	15.37	1.04
		Floor 1	16.69	8.44	25.13	3.16	17.23	1.64
		Floor 2	13.95	4.44	18.40	2.02	17.36	1.18
		Floor 3	16.74	5.40	22.14	2.19	17.23	1.39
		HLC_{sum}	58.94	21.34	80.28	8.76	16.80	5.25
		$HLC_{building}$	58.94	21.34	80.28	8.76	16.86	5.28
	Period 3 16/01/26 19:00 - 15/01/30 20:00	Floor 0	9.26	3.09	12.35	0.90	11.64	1.14
		Floor 1	11.90	8.46	20.36	2.02	13.15	1.70
		Floor 2	9.95	4.27	14.23	1.29	13.57	1.14
		Floor 3	12.51	5.36	17.87	1.39	13.77	1.40
		HLC_{sum}	43.62	21.18	64.81	5.60	13.03	5.38
		$HLC_{building}$	43.62	21.18	64.81	5.62	13.03	5.40
	Period 4 15/02/03 6:00 - 15/02/07 1:00	Floor 0	14.09	3.11	17.20	1.10	17.82	1.03
		Floor 1	18.92	8.46	27.38	2.47	19.52	1.54
		Floor 2	14.95	4.35	19.30	1.57	19.73	1.07
		Floor 3	17.97	5.55	23.52	1.71	19.80	1.28
		HLC_{sum}	65.93	21.47	87.40	6.85	19.22	4.93
		$HLC_{building}$	65.93	21.47	87.40	6.85	19.23	4.94
2015 - 2016	Period 1 15/11/24 19:00 - 15/11/27 22:00	Floor 0	5.82	2.44	8.25	0.47	8.53	1.05
		Floor 1	11.23	7.50	18.72	1.05	11.68	1.73
		Floor 2	9.17	3.98	13.15	0.67	11.83	1.19
		Floor 3	10.40	4.94	15.34	0.73	11.49	1.43
		HLC_{sum}	36.62	18.85	55.47	2.92	10.88	5.39
		$HLC_{building}$	36.62	18.85	55.47	2.92	10.88	5.48
	Period 2 16/01/06 20:00 - 16/01/09 8:00	Floor 0	4.26	2.38	6.65	0.56	6.77	1.06
		Floor 1	5.74	5.84	11.57	1.26	8.01	1.60
		Floor 2	4.81	3.09	7.90	0.80	7.94	1.10
		Floor 3	5.70	4.33	10.03	0.87	8.01	1.41
		HLC_{sum}	20.51	15.64	36.15	3.49	7.69	5.17
		$HLC_{building}$	20.51	15.64	36.15	3.49	7.61	5.21
2016 - 2017	Period 1 16/12/19 12:00:00 - 16/12/22 6:00:00	Floor 0						
		Floor 1	11.68	7.17	18.85	1.74	14.11	1.49
		Floor 2	9.88	4.07	13.96	1.11	14.28	1.08
		Floor 3	12.05	5.01	17.06	1.21	14.20	1.31
		HLC_{sum}	33.61	16.25	49.87	4.07	14.20	3.87
		$HLC_{building}$	33.61	16.25	49.87	4.07	14.20	3.87
	Period 2 17/01/09 18:00:00 - 17/01/12 7:00:00	Floor 0						
		Floor 1	5.58	6.36	11.94	0.76	11.20	1.13
		Floor 2	6.92	3.71	10.63	0.49	11.70	0.95
		Floor 3	7.58	4.50	12.08	0.53	11.20	1.12
		HLC_{sum}	20.08	14.57	34.65	1.78	11.37	3.20
		$HLC_{building}$	20.08	14.57	34.65	1.78	11.36	3.19

Table A.3. Main variables period averaged values for winters 2014-2015, 2015-2016 and 2017-2018 before retrofitting.

Winter	After Retrofitting		Q [kW]	K [kW]	Q+K [kW]	SaVsol ≃ SaHsol [kW]	Tin-Tout [K]	HLC [kW/K]
2017 - 2018	Period 1 17/11/06 18:00- 17/11/10 9:00	Floor 0	6.16	2.04	8.20	2.31	13.74	0.77
		Floor 1	7.64	6.12	13.77	5.20	14.66	1.29
		Floor 2	5.46	3.58	9.03	3.32	14.11	0.88
		Floor 3	3.11	4.63	7.74	3.61	11.81	0.96
		HLC_{sum}	22.37	16.37	38.74	14.44	13.58	3.90
		$HLC_{building}$	22.37	16.37	38.74	14.44	13.58	3.92
	Period 2 17/11/26 21:00- 17/12/02 12:00	Floor 0	8.13	2.14	10.27	1.77	16.99	0.71
		Floor 1	12.75	6.18	18.92	3.97	17.90	1.28
		Floor 2	7.77	3.75	11.52	2.54	18.28	0.77
		Floor 3	7.24	4.86	12.10	2.76	17.33	0.86
		HLC_{sum}	35.88	16.93	52.81	11.04	17.62	3.61
		$HLC_{building}$	35.88	16.93	52.81	11.04	17.62	3.62
	Period 3 17/12/20/ 9:00 - 17/12/23/ 9:00	Floor 0	6.93	2.31	9.25	1.82	14.86	0.75
		Floor 1	10.86	5.69	16.55	4.11	15.61	1.32
		Floor 2	6.47	3.60	10.06	2.62	15.87	0.80
		Floor 3	6.66	5.17	11.82	2.85	15.09	0.97
		HLC_{sum}	30.92	16.76	47.68	11.40	15.36	3.84
		$HLC_{building}$	30.92	16.76	47.68	11.40	15.36	3.85
	Period 4 18/1/17/ 4:00 - 18/1/20/ 6:00	Floor 0	6.99	2.17	9.16	1.84	14.44	0.76
		Floor 1	10.72	5.58	16.30	4.13	15.33	1.33
		Floor 2	7.42	3.30	10.72	2.64	15.50	0.86
		Floor 3	8.03	4.77	12.80	2.87	14.66	1.07
		HLC_{sum}	33.16	15.82	48.98	11.49	14.98	4.03
		$HLC_{building}$	33.16	15.82	48.98	11.49	14.98	4.04
	Period 5 18/2/6/ 17:00- 18/2/10/ 7:00	Floor 0	6.93	2.31	9.25	1.82	14.86	0.75
		Floor 1	10.86	5.69	16.55	4.11	15.61	1.32
		Floor 2	6.47	3.60	10.06	2.62	15.87	0.80
		Floor 3	6.66	5.17	11.82	2.85	15.09	0.97
		HLC_{sum}	30.92	16.76	47.68	11.40	15.36	3.84
		$HLC_{building}$	30.92	16.76	47.68	11.40	15.36	3.85

Table A.4. Main variables period averaged values for winter 2017-2018 after retrofitting.

As can be seen, the period averaged solar gain values are quite low in comparison with the rest of the heat gains inside the building (Q+K). During the last winter, the solar gains weight increased in comparison with the rest of the heat gain inside the building. The method was also able, however, to provide suitable results. Moreover, it can also be seen that, when checking the temperature difference between the interior and the exterior, the obtained value is usually around 15°C.

II. Appendix B

Since one of the method requirements is that the stabilization band of the selected periods in the accumulated average plots should be ± 10% as compared to the HLC estimate during the last 24 hours of the period, the accumulated HLC graphs have been plotted for all floors and for the whole building in all the analysed periods. However, only the most interesting cases have been plotted below:

Winter 2014-2015

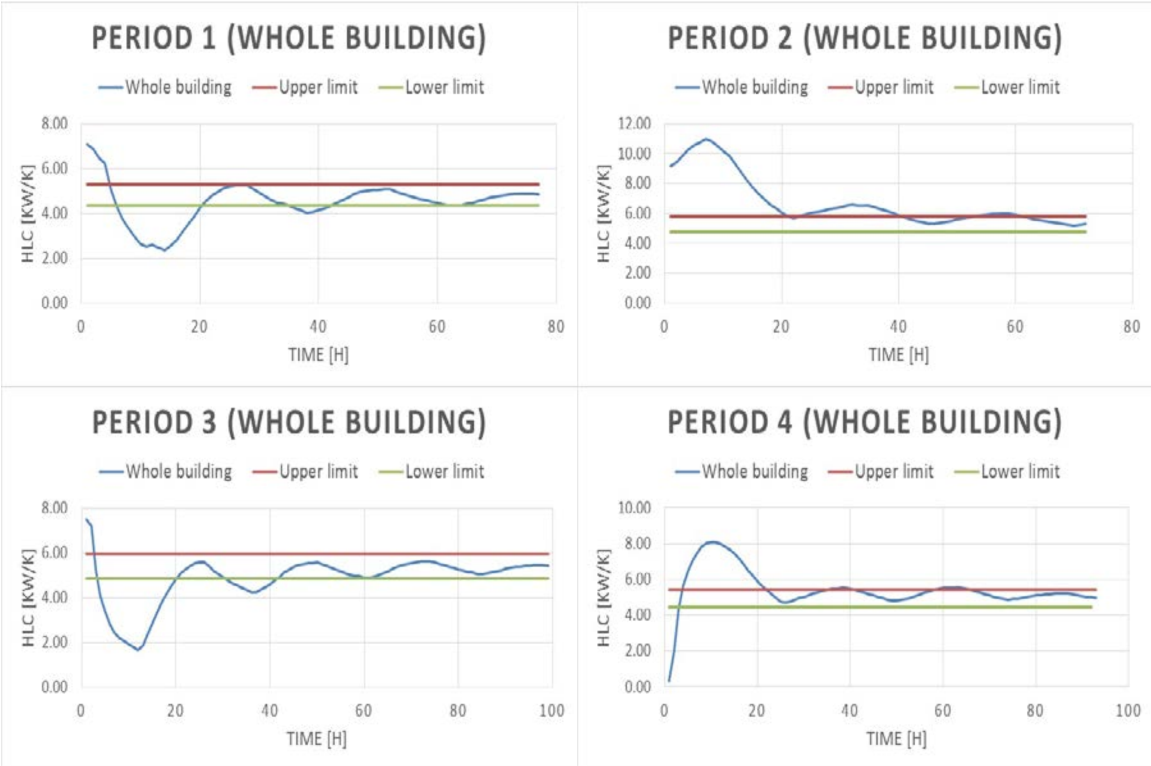

Figure B.1. The accumulated HLC for the whole building for all periods in 2014-2015.

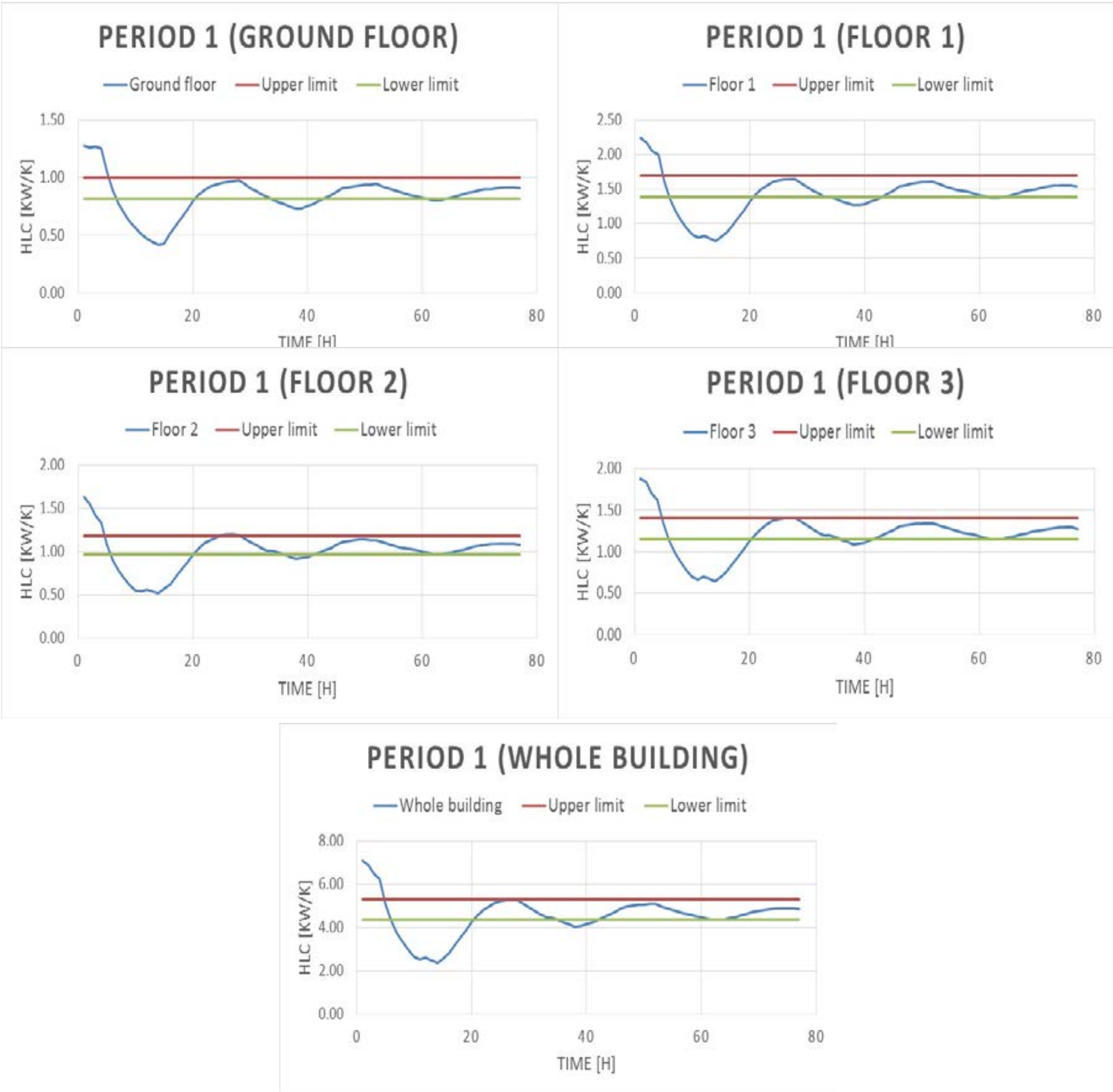

Figure B.2. The accumulated HLC for period one in 2014-2015.

Winter 2015-2016

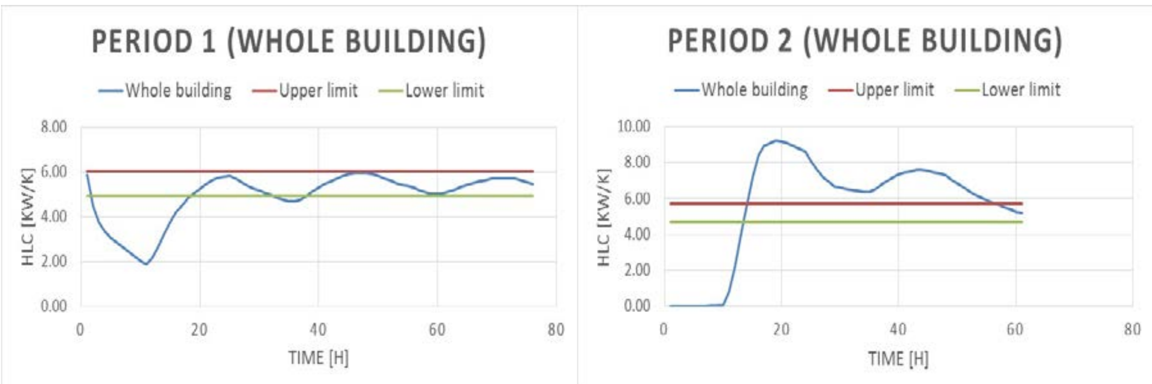

Figure B.3. The accumulated HLC for the whole building for all periods in 2015-2016.

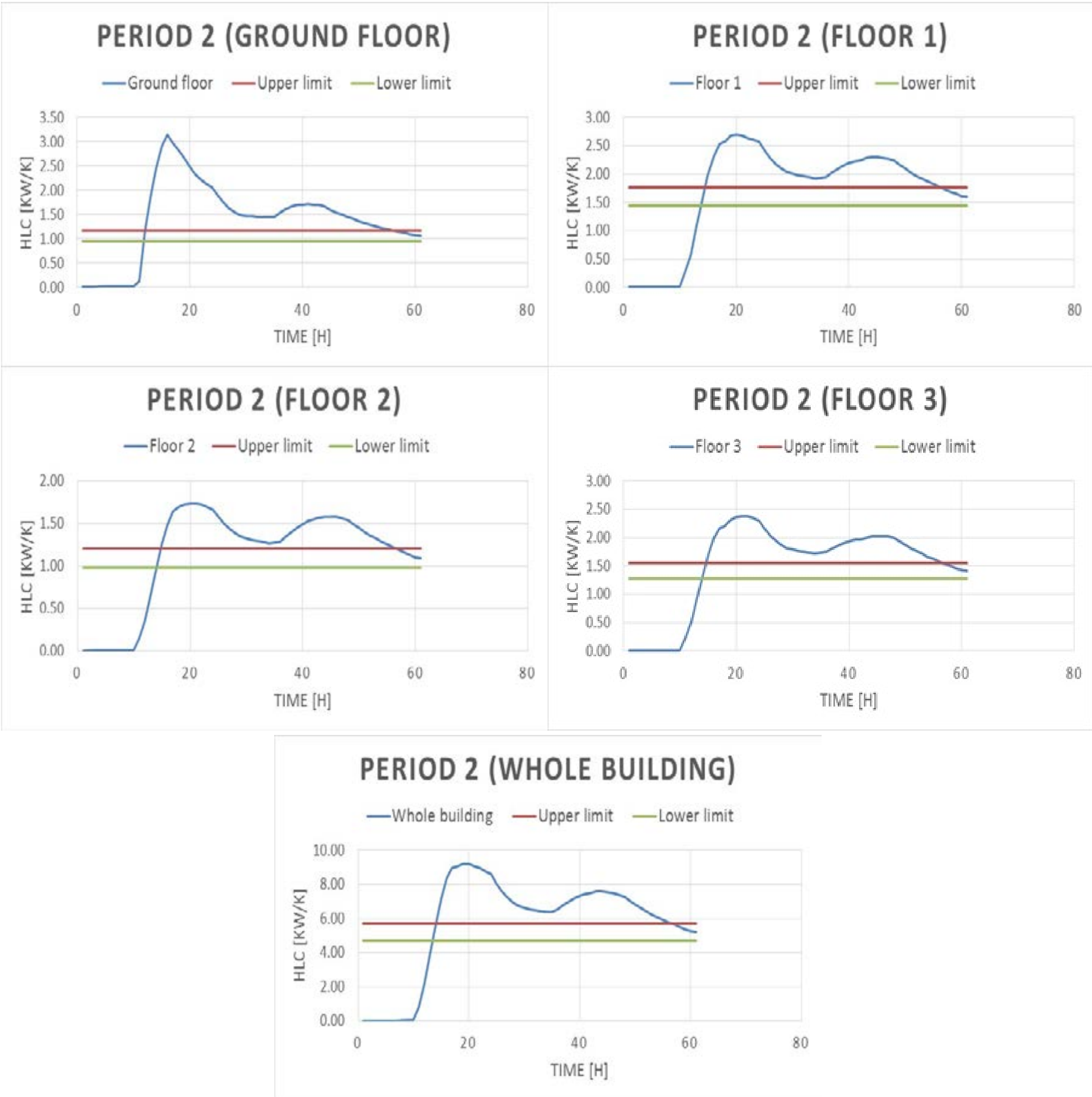

Figure B.4. The accumulated HLC for period two in 2015-2016.

Winter 2016-2017

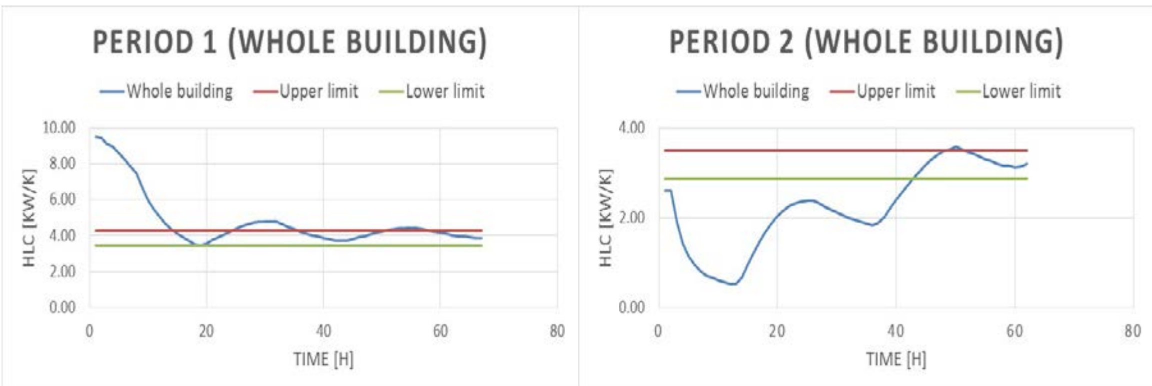

Figure B.5. The accumulated HLC for the whole building for all periods in 2016-2017.

Winter 2017-2018

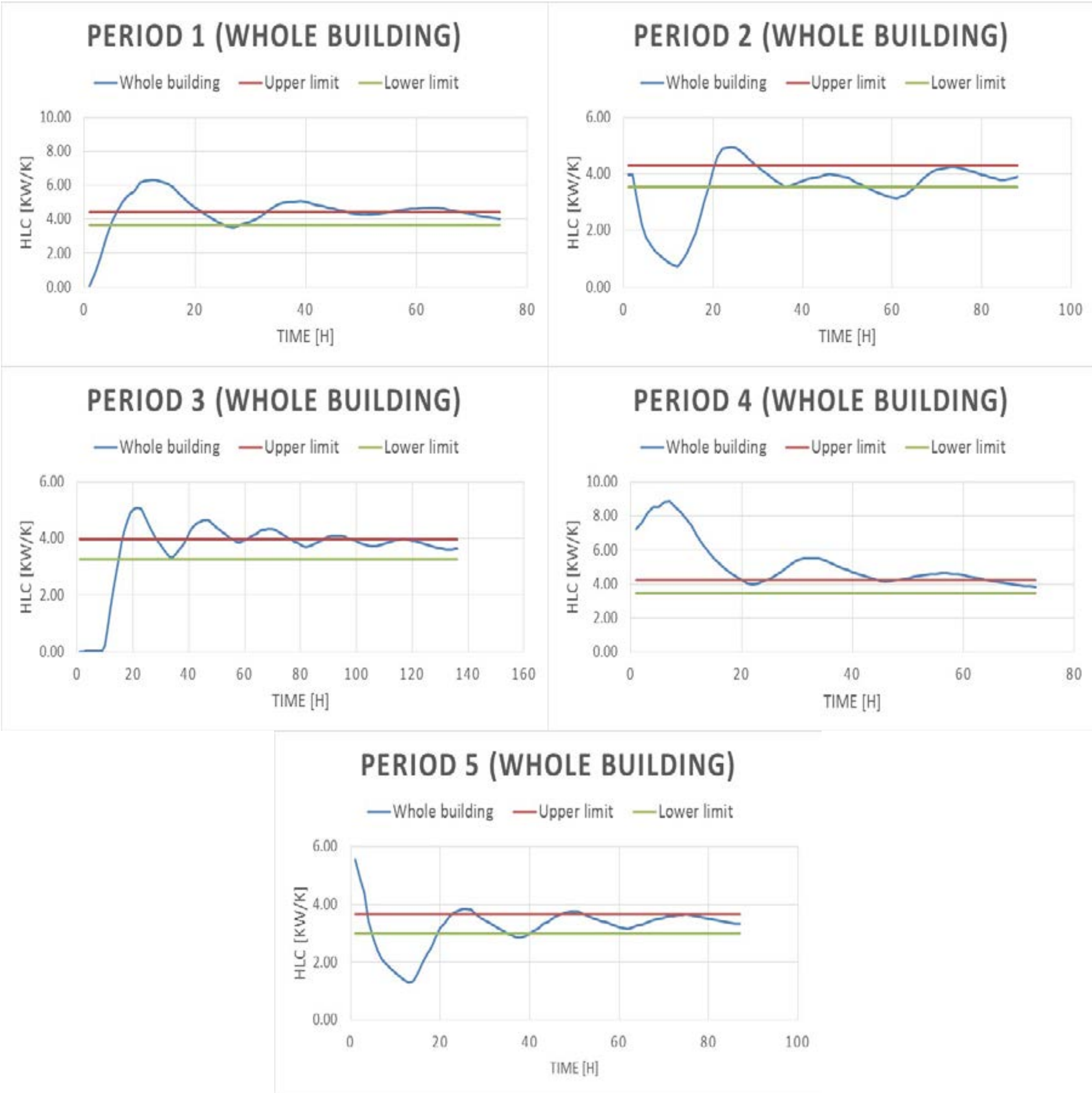

Figure B.6. The accumulated HLC for the whole building for all periods in 2017-2018.

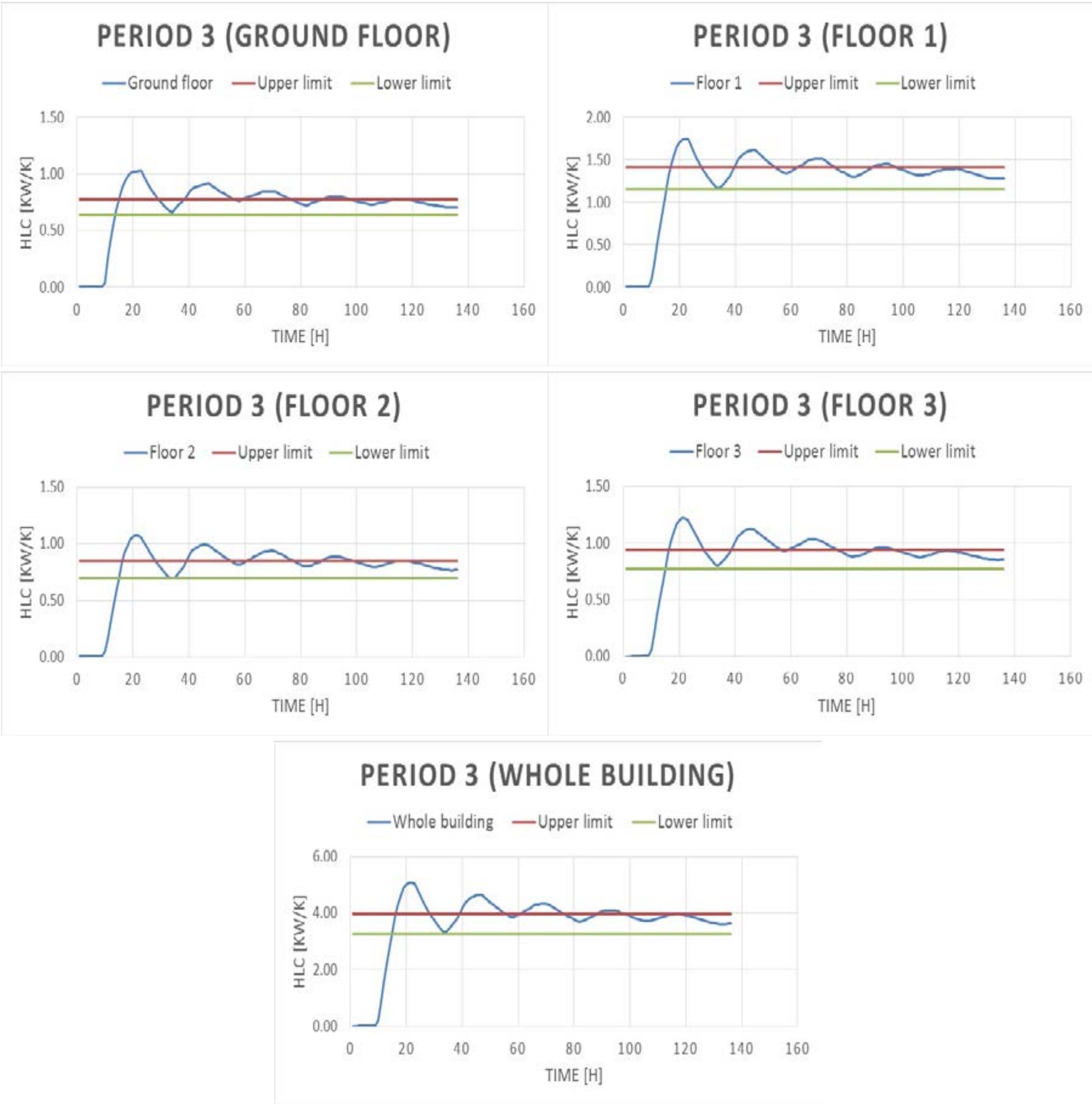

Figure B.7. The accumulated HLC for period three in 2017-2018.

As shown in previous figures, the variation of the accumulated average HLC is considerable until it reaches the last 24 hours. Therefore, it is important to consider only long periods where the accumulated average HLC value is stable during the last 24 hours. A proof of this conclusion can be clearly seen in Figure B.4, where the estimated period is shorter than 72h and not long enough to be stabilized during the last 24 hours. However, during this analysis, the obtained HLC value is considered correct, since it is really close to the HLC values obtained with other periods and it is very close to the minimum period length requirement of 72 hours. On the other hand, the rest of the periods do not show noteworthy issues. The rest of the plots are also available under request to the main author.